PERGAMON

Chemical Engineering Science 58 (2003) 1251–1269

Chemical Engineering Science

www.elsevier.com/locate/ces

Optimal moving and fixed grids for the solution of discretized population balances in batch and continuous systems: droplet breakage

M. M. Attarakih[a], H.-J. Bart[a,*], N. M. Faqir[b]

[a] *Institute of Thermal Process Engineering, Kaiserslautern University, P.O. Box 3049, D-67653 Kaiserslautern, Germany*
[b] *Chemical Engineering Department, University of Jordan, 11942 Amman, Jordan*

Received 13 September 2001; received in revised form 10 July 2002; accepted 12 November 2002

Abstract

The numerical solution of droplet population balance equations (PBEs) by discretization is known to suffer from inherent finite domain errors (FDE). Tow approaches that minimize the total FDE during the solution of discrete droplet PBEs using an approximate optimal moving (for batch) and fixed (for continuous systems) grids are introduced. The optimal grids are found based on the minimization of the total FDE, where analytical expressions are derived for the latter. It is found that the optimal moving grid is very effective for tracking out steeply moving population density with a reasonable number of size intervals. This moving grid exploits all the advantages of its fixed counterpart by preserving any two pre-chosen integral properties of the evolving population. The moving pivot technique of Kumar and Ramkrishna (Chem. Eng. Sci. 51 (1996b) 1333) is extended for unsteady-state continuous flow systems, where it is shown that the equations of the pivots are reduced to that of the batch system for sufficiently fine discretization. It is also shown that for a sufficiently fine grid, the differential equations of the pivots could be decoupled from that of the discrete number density allowing a sequential solution in time. An optimal fixed grid is also developed for continuous systems based on minimizing the time-averaged total FDE. The two grids are tested using several cases, where analytical solutions are available, for batch and continuous droplet breakage in stirred vessels. Significant improvements are achieved in predicting the number densities, zero and first moments of the population.

Keywords: Population balance; Droplet breakage; Moving grid; Optimization; Finite domain error

1. Introduction

In general, the population balance equation (PBE) is a statement of continuity for particulate systems. It represents the net rate of number of particles that are formed by breakage, coalescence, and growth. It is for the sake of mathematical lucidity we define a particle state space continuum that spreads through the internal and external coordinates (Ramkrishna, 1985). By internal coordinates it is meant the variables that describe those quantities associated with the particle, while the term external coordinates is used to denote the position of the particles centre of mass. The population of particles is considered to be large enough so that the random fluctuations in the particle behavior could be averaged out (Mickley, Sherwood, & Reed, 1990; Milton & Arnold, 1990; Ramkrishna, 2000). The population of particles in the particle state space continuum is described by a number density function $n(v,r,t)$, where v and r are the internal and external particle coordinates, respectively, and t is time.

The PBE for a steady and uncompressible flow into a well-stirred vessel could be written as (Barone, Furth, & Loynaz, 1980; Lister, Smit, & Hounslow, 1995; Ribeiro, Regueiras, Guimaraes, Madureira, & Cruz-Pintu, 1995; Ramkrishna, 2000)

$$\frac{\partial n(v,t)}{\partial t}+\frac{\partial[\dot{v}n(v,t)]}{\partial v}=\frac{1}{\tau}(n^{\text{feed}}(v,t)-n(v,t))+\rho[\{n(v,t)\};v,t], \quad (1)$$

where the first term on the left-hand side denotes the rate of accumulation of droplet of size v, the second term is the convective flux along the droplet internal coordinate with a growth velocity $\dot{v}$. The first term on the right-hand side is the net bulk flow into the vessel and the second term is the net rate of droplet generation by coalescence and breakage and is

* Corresponding author. Tel.: +49-631-205-2414; fax: +49-631-205-2119.
E-mail address: bart@mv.uni-kl.de (H.-J. Bart).
URL: http://www.uni-kl.de/LS-Bart/

0009-2509/03/$ - see front matter © 2003 Elsevier Science Ltd. All rights reserved.
doi:10.1016/S0009-2509(02)00654-1

given by (Valentas & Amundson, 1966; Valentas, Bilois, & Amundson, 1966; Kumar, Kumar, & Gandhi, 1993; Kumar & Ramkrishna, 1996a; Podgorska & Baldyga, 2001):

$$\rho[\{n(v,t)\};v,t] = -\Gamma(v)n(v,t) - \int_0^\infty \omega(v,v')n(v,t)n(v',t)\,\mathrm{d}v' + \int_v^\infty \beta(v\,|\,v')\Gamma(v')n(v',t)\,\mathrm{d}v' + \frac{1}{2}\int_0^v \omega(v-v',v')n(v',t)n(v-v',t)\,\mathrm{d}v', \quad (2)$$

where: $\Gamma(v)$ and $\omega(v,v')$ are the breakage and coalescence frequencies, respectively, and $\beta(v\,|\,v')\,\mathrm{d}v$ is the number of droplets having volume in the range v to $v+\mathrm{d}v$ formed upon breakage of droplet of volume v'.

The first two terms represent droplet loss due to breakage and coalescence and the last two terms represent droplet formation due to breakage and coalescence, respectively. Note that the source term, $\rho[\{n(v,t)\};v,t]$, is a functional, rather than a simple function of v and t, but is a function of a whole function $n(v,t)$. Moreover, the function, $\beta(v\,|\,v')$, (sometimes called the daughter droplet distribution) must satisfy the constraints of volume conservation and the average number of daughter droplets produced in a breakage event (Ziff, 1991; Ramkrishna, 2000).

Eqs. (1) and (2) comprise an integro-partial differential equation, which despite its importance rarely has an analytical solution. However, few cases with assumed functional forms of breakage rate, daughter droplet distribution, coalescence kernel functions exist, where most of these solutions are for the batch stirred vessel. (Blatz & Tobolsky, 1945; Scott, 1968; Bajpai & Ramkrishna, 1976; Vigil & Ziff, 1989; Ziff & McGrady, 1985; McGrady & Ziff, 1988; Ziff, 1991).

In general, numerical solutions for Eq. (1) are sought where several methods are proposed in the literature. These methods could be divided into two broad classes (Kostoglou & Karabelas, 1994): zero-order methods, where the internal coordinate is represented by a piecewise constant function and higher-order methods in which higher-order polynomials are used. Kostoglou and Karabelas (1994) evaluated the zero-order methods that are used to solve the coalescence equation in batch vessels and they came to a conclusion that methods conserving droplet number and volume are the most advantageous. Kumar and Ramkrishna (1996a) critically reviewed both methods where they concluded that zero-order methods, containing no double integrals, and conserving both numbers and volumes are not only computationally efficient but also are accurate.

To Hounslow, Ryall, and Marshal (1988) and Hounslow (1990) goes the credit as they took care of preserving both droplet number and volume for coalescence and growth in batch and continuous vessels at steady state using the zero-order method to discretize the PBE. Lister et al. (1995) introduced a discretized PBE for coalescence and growth with an adjustable geometric internal coordinate discretization and thus had overcome the flaw of the fixed geometric internal coordinate of Hounslow et al. (1988). Hill and Ng (1995) have followed Hounslow et al. (1988) in developing a discretized PBE that conserve both number and volume. However, the disadvantage of this method is that it is problem dependent, that is, the discretization coefficients should be derived for each set of breakage functions.

The great achievement made in the discretization of the PBE for batch systems is due to Kumar and Ramkrishna (1996a, b, 1997) where they introduced a general framework of discretization using the zero-order approach. Their method deems internal consistency of any two pre-chosen moments of the population such as number and volume. By internal consistency it is meant that for any two pre-chosen moments of the distribution, there exist two ways to obtain them. The first one is by discretizing the continuous PBE, and the second one is by deriving these moments from the discrete population balance equations (DPBE). The internal consistency is enforced by redistribution of the total property for a droplet between two adjacent representative sizes called the pivots. This concept converts the PBE into set of discrete partial differential equations (with no double integrals) and is called the fixed pivot technique.

The fixed pivot technique has a disadvantage by being inappropriate for predicting steeply changing number densities when coarse grids are used. To preserve the desirable coarseness of the grid, and hence keeping the number of equations as small as possible, it is required to change the position of the pivots in the subsequent intervals to follow these sharp changes in number density. The moving pivot technique of Kumar and Ramkrishna (1996b) comes to accomplish this task. Due to the generality and accuracy of this technique, it will be used in the present work to discretize Eqs. (1) and (2).

Nevertheless, the discretization of the source term given by Eq. (2) is by no means exact, and it is inherently associated with the so-called finite domain error (FDE) (Gelbard & Seinfeld, 1978; Sovova & Prochazka, 1981; Hounslow, 1990; Nicmanis & Hounslow, 1998). This is an inevitable result of trying to use a finite internal droplet coordinate to approximate the infinite one. As so far, only Sovova and Prochazka (1981) tried to investigate rigorously the effect of the FDE on the accuracy of the DPBE when zero-order methods are used. They studied droplet breakage and coalescence in batch vessels at steady state and tried to estimate the FDE by extrapolating both ends of the droplet distribution. The main drawback of this technique is the general uncertainties associated with extrapolation and its lack of general relations to predict the time-dependent FDE. Moreover, since the evolution of the droplet size distribution in batch and continuous systems is a dynamic phenomenon, it is desirable to find out how to minimize the increasing FDE with time. Discretization of the internal droplet coordinate (droplet volume) requires specification of minimum and maximum droplet volumes. This discretization results

in contiguous intervals compromising a grid that covers the specified range.

The objective of this work is to develop an approximate optimal moving gird technique and a time-averaged optimal fixed grid for batch and continuous systems respectively, based on the minimization of the total FDE. The proposed optimal moving grid for droplet breakage in a batch vessel has the advantage of being internally consistent by conserving any two integral properties of the distribution. General equations are also derived for the FDE by approximate discretization of the general PBE. The possibility of solving the resulting DPBEs sequentially in time is also shown. The developed optimal grids are tested using various analytical solutions available in the literature.

2. Discretization of the PBE for continuous systems using the moving pivot technique

In practical applications, often of primary interest are some integral properties of the population rather than the entire population itself. For example in modeling of liquid–liquid dispersion systems, the mean droplet size and the hold up are of primary interest (Garg & Pratt, 1984; Eid, Gourdon, & Casamatta, 1991; Alopaeus, Koskinen, & Keskinen, 1999). However, in this discretization technique it is intended to correctly predict the changes in the required integral properties by exactly preserving the changes of the properties of the single droplets from which the integral ones evolve. This is because the prediction of the number density itself is computationally expensive and contains information more than that is usually required.

To proceed further, let the internal coordinate represents the droplet volume and be discretized according to the partition (grid) $V_M \equiv \{v_0, v_1, \ldots, v_{M+1}\}$, where $v_0 = 0$, $v_1 = v_{\min}$, and $v_M = v_{\max}$. Let the ith interval be denoted by $I_i = [v_i, v_{i+1})$ and the number density function is represented by (Kumar & Ramkrishna, 1996a):

$$n(v,t) = \sum_i N_i \delta(v - x_i), \tag{3}$$

where δ is the Dirac delta function, x_i is the characteristic or representative size of the population in the interval I_i where it is called the pivot and N_i is the discrete number density. The pivots simply concentrate the population in any interval at a single point where their positions are allowed to change, such that the required integral properties are preserved. The positions of these pivots, as we shall see later, are functions of both time and the coalescence and breakage functions. The pivots are dynamic quantities that follow the changes in the number density according to the following relation when the droplets volume is preserved (Kumar & Ramkrishna, 1996b):

$$x_i(t) = \frac{\int_{v_i}^{v_{i+1}} v n(v,t)\,\mathrm{d}v}{\int_{v_i}^{v_{i+1}} n(v,t)\,\mathrm{d}v}, \quad v_i \leqslant x_i < v_{i+1}. \tag{4}$$

This definition of the pivot is consistent with the mean value theorem of integrals such that it moves in the interval as the number density changes. It remains close to v_i for decreasing number density and close to v_{i+1} or to the middle of the interval for increasing and uniform number densities, respectively.

The coefficients N_i resemble the number density function in the interval I_i and are considered functions of time only. These functions represent the total number of droplets in the ith interval and are related to the continuous number density by

$$N_i(t) = \int_{v_i}^{v_{i+1}} n(v,t)\,\mathrm{d}v. \tag{5}$$

In the present work, we will focus on the case of pure breakage in batch and continuous vessels since the coalescence and growth for batch and continuous systems are well-studied (Hounslow et al., 1988; Hounslow, 1990; Lister et al., 1995; Kumar & Ramkrishna, 1996b; Ramkrishna, 2000).

To derive an internally consistent set of DPBE with respect to total number and droplet volume, we follow Kumar and Ramkrishna (1996b), where Eqs. (1) and (2) could be discretized by integrating both sides with respect to v from v_i to v_{i+1} which results in

$$\frac{\mathrm{d}N_i(t)}{\mathrm{d}t} = \lambda_i^c N_i(t) + \sum_{k=i+1}^{M} \pi_{0,i,k} \Gamma_k N_k(t) + \frac{N_i^{\mathrm{feed}}}{\tau}, \quad i = 1, 2, \ldots, M-1, \tag{6}$$

where

$$\Gamma_k = \Gamma(x_k(t)), \tag{7}$$

$$\pi_{0,i,k} = \int_{v_i}^{u_i} \beta(v \mid x_k)\,\mathrm{d}v, \quad \begin{cases} u_i = x_i, & k = i, \\ u_i = v_{i+1}, & k > i, \end{cases} \tag{8}$$

$$\lambda_i^c = \Gamma_i(\pi_{0,i,i} - 1) - \frac{1}{\tau}. \tag{9}$$

Eq. (6) conserves the total number of droplet in the ith interval and is internally consistent with respect to the zero moment of the distribution. To conserve the total droplet volume (mass) in each interval, Eqs. (1) and (2) are written in terms of the volume distribution ($p = vn(v)$) and integrated with respect to v from v_i to v_{i+1}, where after some algebraic manipulation one could obtain

$$\frac{\mathrm{d}x_i(t)}{\mathrm{d}t} = \eta_i + \frac{1}{N_i(t)} \sum_{k=i+1}^{M} (\pi_{1,i,k} - x_i \pi_{0,i,k}) \Gamma_k N_k(t), \quad i = 1, 2, \ldots, M-1, \tag{10}$$

where

$$\eta_i = (\pi_{1,i,i} - x_i \pi_{0,i,i}) \Gamma_i + \frac{x_i^{\mathrm{feed}} - x_i}{\tau} \left(\frac{N_i^{\mathrm{feed}}}{N_i} \right), \tag{11}$$

$$\pi_{1,i,k} = \int_{v_i}^{u_i} v \beta(v \mid x_k)\,\mathrm{d}v, \quad \begin{cases} u_i = x_i, & k = i, \\ u_i = v_{i+1}, & k > i. \end{cases} \tag{12}$$

It should be noted that Eq. (10) becomes independent of the feed droplet distribution, N^{feed}, as well as the vessel residence time τ in case of sufficiently fine discretization ($x_i^{\text{feed}} \approx x_i$), which is a desirable result. This is really the same equation for batch vessels derived by Kumar and Ramkrishna (1996b) when $N_i^{\text{feed}} \to 0$. Eqs. (6) and (10) comprise a system of ordinary differential equations describing the evolution of the discrete number density through estimating the total number and volume of droplets in the ith interval with the desired accuracy. To completely specify this system, the following two sets of initial conditions are stipulated:

$$N_i(0) = N_i^0,$$
$$x_i(0) = x_i^0, \quad i = 1, 2, \ldots, M-1. \tag{13}$$

3. Error of discretization

In discretizing an equation defined over an infinite domain, an inherent error is incurred due to the failure of taking into account the portion of the function lying outside the domain of discretization. This type of error is termed FDE (Gelbard & Seinfeld, 1978; Hounslow, 1990), and as a result it causes a nonzero lower and upper residuals below and above the discrete limits of integration. These lower (FDE^L) and upper (FDE^U) residuals represent cumulative number densities that are given by (Sovova & Prochazka, 1981)

$$\text{FDE}_0^L(v_{\min}, t) = \int_0^{v_{\min}} n(v,t)\,\mathrm{d}v, \tag{14}$$

$$\text{FDE}_0^U(v_{\max}, t) = \int_{v_{\max}}^{\infty} n(v,t)\,\mathrm{d}v, \tag{15}$$

where the subscript zero is used to refer to the residuals of the zero moment of the distribution. This choice is actually suitable for characterizing the FDE since in droplet breakage a large number of droplets having a small volume is produced as breakage proceeds. So, these lower and upper residuals could be related to the total number of droplets for the continuous distribution as follows:

$$N^c(t) = \text{FDE}_0^L(v_{\min}, t) + \sum_{i=1}^{M-1} \int_{v_i}^{v_{i+1}} n(n,t)\,\mathrm{d}v + \text{FDE}_0^U(v_{\max}, t). \tag{16}$$

The discrepancy between the continuous number of droplets, $N^c(t)$, at any instant of time and its discrete counterpart, $N^d(v_{\min}, v_{\max}, t)$, could be interpreted by defining the so-called error of discretization. The error of discretization, ε_0, is defined as the difference of sums between the continuous and discrete number of droplets for the intervals $(0, \infty)$ and $[v_{\min}, v_{\max}]$, respectively:

$$\varepsilon_0(t) = N^c(t) - \sum_{i=1}^{M-1} N_i(t). \tag{17}$$

By combining the last two equations, the error of discretization becomes

$$\varepsilon_0(t) = \text{FDE}_0^L(v_{\min}, t) + \text{FDE}_0^U(v_{\max}, t). \tag{18}$$

This result shows that the discretization error in the number of droplets is solely due to the total FDE comprising of the sum of both the lower and upper residuals defined by Eqs. (14) and (15). This means that even for an exact number of droplets, and by excluding the integration error induced by discretization, the total FDE will never be zero as long as a finite domain is considered. Moreover, for a given number of intervals, M, and interval width, Δv, the total FDE at any instant of time is a function only of $v_{\min}$. Since the lower residual decreases as $v_{\min}$ decreases and the upper residual increases at the same time, then there exist due to these opposing effects an optimal minimum droplet volume that minimizes the sum of both residuals. This means as far as discrete distribution is considered, a choice of $v_{\min}$, below the optimal value will increase the discretization error in opposite to the general intuition that decreasing $v_{\min}$ will improve the solution. Actually, Hounslow (1990) showed that when a value of minimum droplet volume is chosen below the optimal one, an artifact oscillation in N_i is observed in the few first number of intervals.

To find the optimal minimum droplet volume that minimizes the total FDE, it is sufficient to differentiate Eq. (18) with respect to $v_{\min}$ at given M and Δv. By using the definition of the residuals (Eqs. (14) and (15)) and making use of Leibnitz formula (Mickley et al., 1990) one could obtain

$$n(v_{\min}^*, t) - \frac{\mathrm{d}v_{\max}}{\mathrm{d}v_{\min}}\, n(v_{\max}^*, t) = 0 \tag{19}$$

and the discrete counterpart of Eq. (19) is

$$\frac{\bar{N}_0^*(t) + \bar{N}_1^*(t)}{2} - \frac{\mathrm{d}v_{\max}}{\mathrm{d}v_{\min}} \left(\frac{\bar{N}_{M-1}^*(t) + \bar{N}_M^*(t)}{2} \right) = 0, \tag{20}$$

where the number densities $n(v_{\min}^*, t)$ and $n(v_{\max}^*, t)$ are approximated by the arithmetic of their average discrete values at the adjacent intervals I_0, I_1 and I_{M-1}, I_M, respectively (Marchal, David, Klein, & Villermaux, 1988). Note that the maximum droplet volume must be a continuous function of $v_{\min}$ in order to satisfy the conditions implied by Eqs. (22) and (23). As will be shown later, a geometric grid with adjustable geometric factor, $\sigma > 1$, will be a suitable choice for the discretization of the droplet internal coordinate (v):

$$v_{\max} = \sigma^{M-1} v_{\min}. \tag{21}$$

It should be noted that the discretization parameters are: the total number of intervals, M, the optimal minimum droplet volume, $v_{\min}^*$, and the interval width controlled by the geometric factor σ.

Since the continuous and discrete number densities appearing in Eqs. (19) and (20), respectively, are functions of time, it follows that the optimal minimum droplet volume, $v_{\min}^*$ is also a function of time. This means that as breakage proceeds to produce smaller number of droplets, the optimal

minimum droplet volume must decrease to account for the increasing number density at the lower size range. At the same time, and due to the conservation of droplet volume, the number density function decreases for large droplets leading to empty classes at the upper size range. This suggests the use of optimal moving grid for droplet breakage in batch vessels, which moves from the upper size range to the lower size range as function of time. To find such an optimal moving grid, Eqs. (6) (for batch), (10), and (20) must be solved simultaneously at each instant of time leading to a differential algebraic system of equations (DAE). Unfortunately, the solution is iterative by starting with an initial guess for the minimum droplet volume at given number of intervals, M, and geometric factor σ followed by solving the system of ODEs (6) and (10). If Eq. (20) is not satisfied, then an improved guess must be used until convergence at each instant of time is achieved. This algorithm seems to be time consuming since it involves solving $2M$ ODEs per iteration at each instant of time and might mask the benefits gained by using the optimal moving grid. To compensate for this drawback, an approximate optimal moving grid technique is derived in the following section.

4. An approximate optimal moving grid technique for batch systems

We return back to the definitions of the lower and upper residuals given by Eqs. (14) and (15) and the definition of the total FDE given by Eq. (18). Since the lower residual decreases as minimum droplet volume increases, and the upper residual increases at the same time, it follows that the total FDE will be close to the minimum value when both residuals are equal (Sovova & Prochazka, 1981). Using this principle, it is possible to force these residuals to be equal at each instant of time and hence producing a minimum droplet volume profile that is close to the exact optimal one. Since the optimal moving grid should keep the number of intervals, and hence the number of DPBE associated with it constant during grid movement, the redistribution of the population between the old and the newly formed grid must conserve any two chosen integral properties of the population. However, we will restrict our attention to the total number and volume in this work (zero and first moment of the population). Now consider the geometric grid shown in Fig. 1 at two instants of time: t and $t+\Delta t$ where the minimum droplet volume moves from $v^*_{\min}(t)$ to $v^*_{\min}(t+\Delta t)$. Let $\gamma_i^{\langle i\rangle}(t)$ be the fraction of droplets at the pivot $x_i(t)$ to be assigned to the pivot $x_i(t+\Delta t)$ and $\gamma_{i+1}^{\langle i\rangle}(t)$ be the fraction of droplets at the pivot $x_i(t)$ to be assigned to the pivot $x_{i+1}(t+\Delta t)$. To conserve both number and volume of these droplets at the ith pivot after redistribution, the following two constraints are set up (refer to Fig. 1b) (Kumar & Ramkrishna, 1997):

$$\gamma_i^{\langle i\rangle} + \gamma_{i+1}^{\langle i\rangle} = 1, \tag{22}$$

$$x_i(t+\Delta t)\gamma_i^{\langle i\rangle} + x_{i+1}(t+\Delta t)\gamma_{i+1}^{\langle i\rangle} = x_i(t). \tag{23}$$

Solving these equations for $\gamma_i^{\langle i\rangle}(t)$ results in

$$\gamma_i^{\langle i\rangle:} = \frac{x_{i+1}(t+\Delta t) - x_i(t)}{x_{i+1}(t+\Delta t) - x_i(t+\Delta t)}. \tag{24}$$

Similar equations could be written for the droplet population at the $(i-1)$th pivot where $\gamma_i^{\langle i-1\rangle}(t)$ is the fraction of droplet at the $x_{i-1}(t)$ pivot assigned to the $x_i(t+\Delta t)$ pivot, and $\gamma_{i-1}^{\langle i-1\rangle}(t)$ is the fraction of droplets at the $x_{i-1}(t)$ pivot assigned to the $x_{i-1}(t+\Delta t)$. Solving these equations yields an expression for $\gamma_i^{\langle i-1\rangle}(t)$:

$$\gamma_i^{\langle i-1\rangle:} = \frac{x_{i-1}(t) - x_{i-1}(t+\Delta t)}{x_i(t+\Delta t) - x_{i-1}(t+\Delta t)}. \tag{25}$$

Now by referring to Fig. 1b, we could obtain the net discrete density of droplet population at the instant $t+\Delta t$ at the new grid from that at the old one at time t using Eqs. (24) and (25)

$$N_i(t+\Delta t) = \gamma_i^{\langle i-1\rangle} N_{i-1}(t) + \gamma_i^{\langle i\rangle} N_i(t), \quad i = 1,2,\ldots,M. \tag{26}$$

When $i=1$, the last equation becomes function of $N_0(t)$ which is not defined by any of the system of Eqs. (6). It is interesting to note that by definition, $N_0(t)$, is the lower residual defined by Eq. (14), and hence its estimation becomes an inevitable necessity for both $N_1(t+\Delta t)$ and the FDE_0^L. The estimation of $N_0(t)$ from the discrete number density will follow in the next section.

Now we shall turn our attention to force both residuals to be equal at any instant of time $t+\Delta t$ utilizing the redistribution concept above. At the time instant $t+\Delta t$ the discrete lower residual of the distribution is found from Eq. (26)

$$\mathrm{FDE}_0^L(t+\Delta t) = \gamma_0^{\langle 0\rangle} N_0(t) \tag{27}$$

and similarly the discrete upper residual is given by

$$\mathrm{FDE}_0^U(t+\Delta t) = \sum_{i=M}^{\infty} \gamma_i^{\langle i-1\rangle} N_{i-1}(t) + \gamma_i^{\langle i\rangle} N_i(t). \tag{28}$$

It could be shown that only the Mth term in the summation above has a significant value since the population contained in the interval $[V_{M+1},\infty)$is approximately negligible for sufficiently large M or geometric factor σ. This is because during droplets breakage the final intervals (numbering is started from the small size to large size) become gradually empty as breakage progresses. Actually, after sufficient time the last interval becomes completely empty and the zero interval is occupied by the newly birthed population of droplets. Moreover, if the initial minimum and maximum droplets sizes are chosen to be optimal according to Eq. (19), then the higher terms in Eq. (28) will be insignificant for sufficiently large M or σ. This is actually equivalent to neglecting droplet breakage from the $(M+1)$th intervals and the higher ones.

The necessary condition for optimality stated by Eq. (19) or (20) is approximately satisfied if both residuals are equal at each instant of time. To accomplish this, we force both

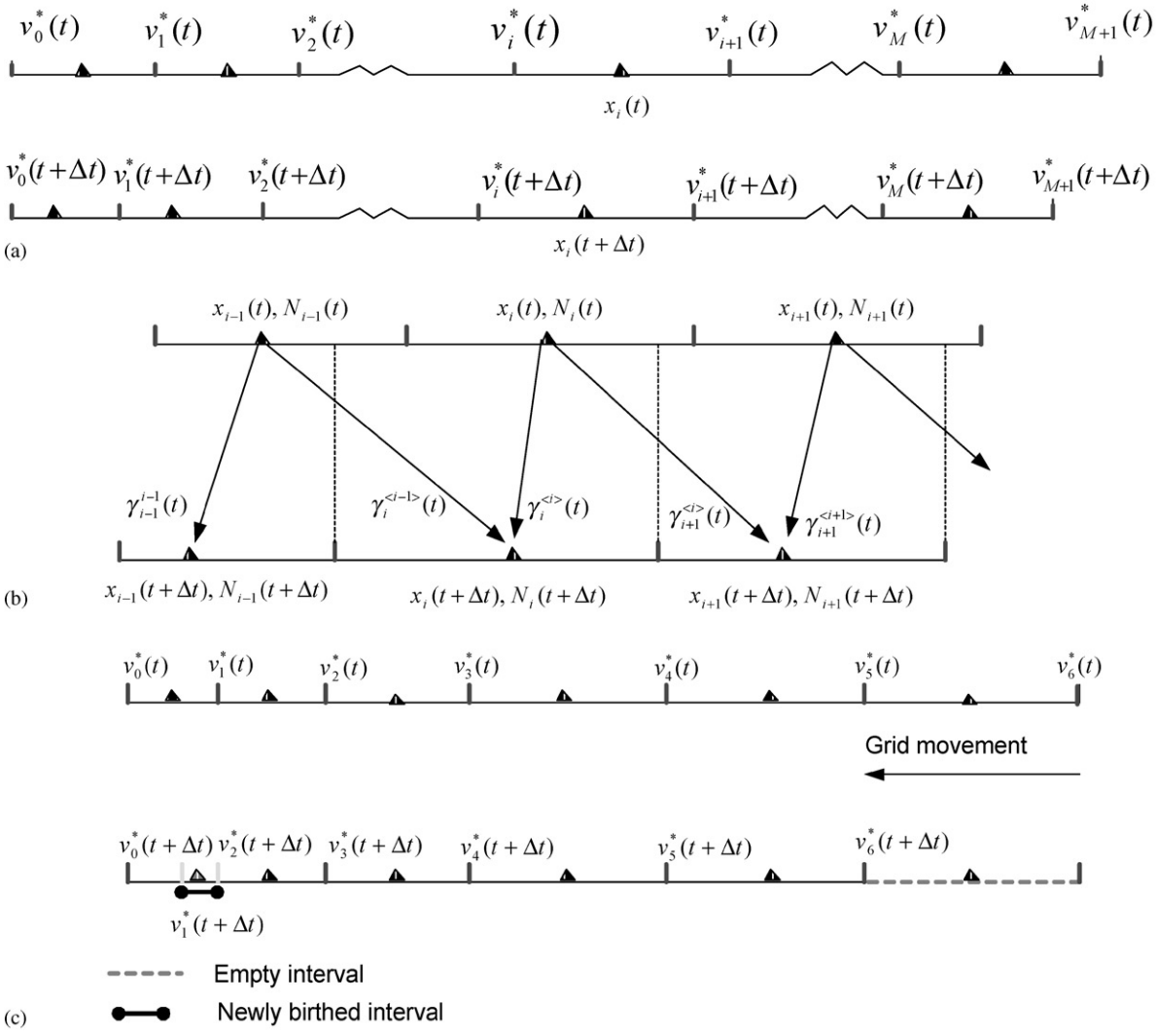

Fig. 1. Typical moving grid.

sides of Eqs. (27) and (28) to be equal, which after some algebraic manipulation yields:

$$\frac{v^*_{\min}(t+\Delta t)}{v^*_{\min}(t)} = \frac{(1/(\sigma-1))N_{M-1}(t)+(1/\sigma)N_0(t)}{((\sigma+1)/\sigma)N_0(t)+(1/(\sigma-1))N_{M-1}(t)-N_M(t)} \tag{29}$$

with $v^*_{\min}(0)$ found from the initial number density and Eq. (19). Eq. (29) specifies the path that must be followed by the grid in order to keep the total FDE approximately minimum based on the zero moment of the distribution.

Since the interval boundaries are now functions of time, then the population contained in it changes also with time. It follows that the discretization of the left-hand side of Eq. (1) for a batch system will be different from that used in the case of a fixed grid. This could be shown by multiplying both sides of Eq. (1) by $\mathrm{d}v$ and integrating over the size range $[v_i(t), v_{i+1}(t)]$:

$$\frac{\partial}{\partial t}\int_{v_i(t)}^{v_{i+1}(t)} n(v,t)\,\mathrm{d}v = \lambda^c_i N_i(t) + \sum_{k=i+1}^{M} \pi_{0,i,k}\Gamma_k N_k(t). \tag{30}$$

By expanding the left-hand side using the Leibnitz formula (Mickley et al., 1990), and noting that the right-hand side involves integration with respect to volume only, one could obtain

$$\int_{v_i(t)}^{v_{i+1}(t)} \frac{\partial n(v,t)}{\partial t}\,\mathrm{d}v + n(v_{i+1}(t),t)\frac{\mathrm{d}v_{i+1}(t)}{\mathrm{d}t} - n(v_i(t),t)\frac{\mathrm{d}v_i(t)}{\mathrm{d}t} = \lambda^c_i N_i(t) + \sum_{k=i+1}^{M} \pi_{0,i,k}\Gamma_k N_k(t). \tag{31}$$

Note that the entire grid boundaries move at the same velocity, that is,

$$\frac{\mathrm{d}v_i(t)}{\mathrm{d}t} = \frac{\mathrm{d}v_{i+1}(t)}{\mathrm{d}t} = \frac{\mathrm{d}v(t)}{\mathrm{d}t}. \tag{32}$$

Using the above relation, Eq. (31) after some algebraic manipulation simplifies to

$$\int_{v_i(t)}^{v_{i+1}(t)} \left[\frac{\partial n(v,t)}{\partial t} + \frac{\mathrm{d}v}{\mathrm{d}t}\frac{\partial n(v,t)}{\partial v}\right] \mathrm{d}v = \lambda_i^c N_i(t) + \sum_{k=i+1}^{M} \pi_{0,i,k}\Gamma_k N_k(t). \quad (33)$$

The term in the brackets on the left-hand side is merely the total derivative of the number density, which describes the change in the number density of size v as noticed by an observer moving with a velocity the same as that of the grid. Using this fact Eq. (33) simplifies to

$$\frac{\mathrm{d}N_i(t)}{\mathrm{d}t} = \lambda_i^b N_i(t) + \sum_{k=i+1}^{M} \pi_{0,i,k}\Gamma_k N_k(t), \quad i = 1,2,\ldots,M-1, \quad (34)$$

where λ_i^b is found from λ_i^c by setting $\tau \to \infty$.

Similarly, the equations of the pivots are still given by Eq. (10) with $\eta_i^b = \lim_{\tau\to\infty} \eta_i^c$, where the change in the position of the pivot in any size range is now with respect to the moving grid.

The set of Eqs. (10), (24)–(26), (29), (34), and the initial conditions specified by Eq. (13) comprise a DAE that could be solved sequentially in time.

The notation will be greatly simplified if these equations are written in a compact matrix form as follows:

$$\frac{\mathrm{d}\boldsymbol{N}}{\mathrm{d}t} = \boldsymbol{A}\boldsymbol{N}, \quad (35)$$

$$\frac{\mathrm{d}\boldsymbol{x}}{\mathrm{d}t} = \boldsymbol{F}(\boldsymbol{x},\boldsymbol{N}), \quad (36)$$

$$\boldsymbol{N}(t+\Delta t) = \boldsymbol{\gamma}(t)\boldsymbol{N}(t) + \boldsymbol{N}_0^{\mathrm{T}}(t)\boldsymbol{\gamma}_0(t), \quad (37)$$

$$\boldsymbol{N}(0) = [N_1(0) \quad N_2(0) \quad \cdots \quad N_{M-1}(0) \quad N_M(0)]^{\mathrm{T}}, \quad (38)$$

$$\boldsymbol{x}(0) = [x_1(0) \quad x_2(0) \quad \cdots \quad x_{M-1}(0) \quad x_M(0)]^{\mathrm{T}}, \quad (39)$$

where $\boldsymbol{A}$ and $\boldsymbol{F}$ are $M \times M$ upper triangular matrices whose elements are given by

$$A_{i,k} = \begin{cases} \lambda_i^b, & k = i, \\ \pi_{0,i,k}\Gamma_k, & k > i, \end{cases} \quad (40)$$

$$F_{i,k} = \begin{cases} \eta_i^b, & k = i, \\ \dfrac{(\pi_{1,i,k} - x_i\pi_{0,i,k})\Gamma_k N_k(t)}{N_i(t)}, & k > i \end{cases} \quad (41)$$

and $\boldsymbol{\gamma}$ is an $M \times M$ bidiagonal matrix whose elements are given by

$$\gamma_{i,k} = \begin{cases} \gamma_i^{\langle i\rangle}, & k = i, \\ \gamma_i^{\langle i-1\rangle}, & k = i-1,\ k \neq 0, \end{cases} \quad (42)$$

$\boldsymbol{\gamma}_0$ and $\boldsymbol{N}_0$ are $M \times 1$ vectors whose elements are

$$\boldsymbol{\gamma}_0 = [\gamma_1^0 \quad 0 \quad \cdots \quad 0 \quad 0)]^{\mathrm{T}}, \quad (43)$$

$$\boldsymbol{N}_0 = [N_0 \quad 0 \quad \cdots \quad 0 \quad 0)]^{\mathrm{T}}. \quad (44)$$

In the above system of equations, the only undetermined variables are $N_0(t)$ and $N_M(t)$ and their corresponding pivots (x_0 and x_M) which will be considered in the next section.

5. Estimation of the lower and upper residuals

It should be clear that in the derivation of the DPBE, the droplets having volume less than $v_{\min}$ have zero breakage frequency. This corresponds to the case of limited breakage, where physically stable minimum droplet volume exists below which no further breakage occurs (Valentas et al., 1966; Tsouris & Tavlarides, 1994; Hill & Ng, 1995; Alopaeus et al., 1999). As the breakage proceeds the optimal minimum droplet volume $v_{\min}^*(t)$ will move toward $v_{\min}$ until both droplet volumes coincide. For the case of full breakage, all the droplets have a nonzero breakage frequency and hence $v_{\min} \to 0$. The discrete droplet population density in the intervals $(0, v_{\min}^*(t)]$ and $[v_{\min}, v_{\min}^*(t)]$, for the case of full and limited breakage, respectively, represents the lower residual or strictly speaking $N_0(t)$. To estimate this population density, Sovova and Prochazka (1981) used a two point linear extrapolation to estimate the steady-state lower residuals in batch vessel where both breakage and coalescence mechanisms were active. Their extrapolation technique is usually useful for nonsteep number densities and might lead to significant erroneous predictions for very steep number densities for which the approximate optimal moving grid technique is developed. Instead of extrapolation, which has considerable numerical uncertainties (Mickley et al., 1990), a natural approximate extension of the discrete equations to include either of the intervals $(0, v_{\min}^*(t)]$ and $[v_{\min}, v_{\min}^*(t)]$ will be used. It could be assumed that either of the aforementioned intervals will only receive broken droplets from higher ones or from droplets within the intervals themselves, and no droplet will be lost through breakage from these intervals (Laso, Steiner, & Hartland, 1987; Hill & Ng, 1995). As a consequence of this assumption, an unsteady-state number balance on these intervals will produce the required differential equation describing the change of $N_0(t)$ with time:

$$\frac{\mathrm{d}N_0(t)}{\mathrm{d}t} = \vartheta(v_{\min}^*(t))\Gamma_0 N_0(t) + \sum_{k=1}^{M} \pi_{0,0,k}\Gamma_k N_k(t). \quad (45)$$

Here $\vartheta(v_{\min}^*)$ is the average number of droplets produced due to the breakage of droplet of volume $v_{\min}^*(t)$.

Since the width of the intervals $(0, v_{\min}^*(t)]$ or $[v_{\min}, v_{\min}^*(t)]$ is very small due to the geometric grid used in discretization, the pivot $x_0(t)$ is fixed at the middle of these intervals without introducing appreciable errors. This is in general always correct when fine grids are used, where it is possible for the fixed pivots to replace the moving ones, that is,

the moments of the population could be predicted without appreciable errors (Ramkrishna, 2000).

To estimate the discrete population density $N_M(t)$, we shall follow the same reasoning used to obtain $N_0(t)$. There are only droplets vanishing from the I_M interval to the lower ones, and formation of droplets by breakage within the Mth interval itself is permitted (Laso et al., 1987; Hill & Ng, 1995). An unsteady-state number balance on the I_M interval results in

$$\frac{dN_M(t)}{dt} = \lambda_M^b N_M(t). \tag{46}$$

Using similar argument, the Mth pivot follows from Eq. (10):

$$\frac{dx_M(t)}{dt} = \eta_M. \tag{47}$$

Eqs. (27) and (28) along with Eqs. (45) through (47) define completely the lower and upper residuals at any instant of time for specified grid parameters σ and M.

6. Sequential solution of the number density and pivot equations

The system of equations for the discrete number density and the pivots given by Eqs. (35) and (36) could be solved sequentially in time. The sequential solution starts by first integrating the number density equations over the time interval $t \in [t, t+\Delta t]$ followed by the integration of the pivot equations. This method of solution is allowed only if the pivots change slowly when compared to the variation of the number densities over sufficiently small interval of time, and hence making the matrices $\boldsymbol{A}$ and $\boldsymbol{F}$ approximately time independent. This is actually valid if the value of the ratio of each time constant of the pivot and number density equations is a large number. Actually, the time constants of Eqs. (6) and (10) are the reciprocal of the eigenvalues of their matrices $\boldsymbol{A}$ and $\boldsymbol{F}$. Since these matrices are both upper triangular, it can be simply shown that their eigenvalues are given by their diagonal elements (Gerald & Wheatly, 1994). The time constants of the present systems are $|\lambda_i^b|^{-1}$ and $|\eta_i|^{-1}$ ($i = 1, 2, \ldots, M$) for number density and pivots, respectively. Accordingly, the condition stated above for the possibility of sequential solution could be written mathematically as

$$\frac{|\eta_i|^{-1}}{|\lambda_i^b|^{-1}} \gg 1. \tag{48}$$

This condition could be satisfied for sufficiently fine grids by using an optimal moving geometric grid. This grid becomes gradually fine as the breakage progresses in time by moving to the left to accommodate the evolving population in the small size range. By applying the mean value theorem of integrals to the system of Eqs. (9) and (11) it is easy to show that

$$\lim_{\Delta v_i \to 0} \frac{|\eta_i|^{-1}}{|\lambda_i^b|^{-1}} \to \infty. \tag{49}$$

This insures the validity of the method of sequential solution in time proposed above. Actually, the system of equations given by Eq. (35) has an explicit solution that is given by

$$\boldsymbol{N}(t) = \boldsymbol{R}\boldsymbol{D}\boldsymbol{R}^{-1}\boldsymbol{N}(0), \tag{50}$$

where $\boldsymbol{D}$ is an $M \times M$ diagonal matrix given by: $\boldsymbol{D} = \mathrm{diag}(e^{\lambda_i^b t})$, $i = 1, 2, \ldots, M$, and $\boldsymbol{R}$ is an $M \times M$ matrix whose columns are the eigenvectors of $\boldsymbol{A}$.

7. The geometric grid

The use of geometric grid in the discretization of the PBEs is extensively used in the literature and its many advantages are found elsewhere (Bleck, 1970; Laso et al., 1987; Hounslow et al., 1988; Lister et al., 1995; Hill & Ng, 1995; Ramkrishna, 2000). However, it is worthwhile to mention two distinctive advantages of the geometric grid that are utilized in this work. The first one is that the geometric grid becomes fine as the entire grid moves to the left and thus allowing steep number density to be correctly tracked out. The second advantage, and the most important, is that when the last grid boundary coincide exactly with $v_{\max}$ due to the grid movement, the new and the old interval boundaries completely coincide except for the first boundary ($v_1(t+\Delta t) = v^*_{\min}(t)$) (see Fig. 1c). This means that the old and the new population densities have the same intervals to occupy, resulting in an exact match between them ($\boldsymbol{N}(t+\Delta t) = \boldsymbol{N}(t)$) but only for the first interval ($N_1(t+\Delta t) = \gamma_1^{\langle 0 \rangle} N_0(t)$). This suggests that the number densities could be updated only when $v^*_{M+1}(t+\Delta t)$ is less than or equal to $v_{\max} = v^*_M(t)$ to exclude any numerical inaccuracies due to population redistribution. However, if the equality is not exactly satisfied, the new pivots are set equal to the old ones since for sufficiently small time step $v^*_{M+1}(t+\Delta t)$ is not greatly different from $v^*_M(t)$. At the same time, the pivot of the newly birthed interval is set at the middle since the width of this interval is very small thanks to the geometric grid. It follows then the stepwise redistribution of the discrete population density will result in an approximate optimal piecewise constant minimum droplet volume profile as a function of time. In fact, this strategy is adopted in the following solution algorithm.

8. Solution algorithm

The solution algorithm using the optimal moving grid could be summarized as follows:

1. Specify σ, M, Δt, t_f and the initial condition $n(v, 0)$.
2. Set $t_0 = 0$.

3. Calculate the discrete initial conditions $\boldsymbol{N}(0)$ and $\boldsymbol{x}(0)$ using Eqs. (5) and (4) and $n(v,0)$.
4. Calculate the initial optimal droplet volume, $v^*_{\min}(0)$, using Eq. (19) and $n(v,0)$.
5. Calculate $\boldsymbol{N}(t_0+\Delta t)$ using Eq. (50) and $\boldsymbol{x}(t_0+\Delta t)$ using Eq. (36) sequentially in time.
6. Calculate $N_0(t_0+\Delta t)$ using Eq. (45).
7. Calculate the optimal droplet volume, $v^*_{\min}(t_0+\Delta t)$, using Eq. (29) and $v^*_{M+1}(t_0+\Delta t)=\sigma^M v^*_{\min}(t_0+\Delta t)$.
8. If $v^*_{M+1}(t_0+\Delta t)\leqslant v^*_M(t_0)$ then:
   8.1. Calculate $v^*_i(t_0+\Delta t)=\sigma^{i-1}v^*_{\min}(t_0+\Delta t)$ for $i=1,2,\ldots,M+1$,
   8.2. Calculate $x_i(t_0+\Delta t)=(v^*_i(t_0+\Delta t)+v^*_{i+1}(t_0+\Delta t))/2$, $i=0,1$, and $x_i(t_0+\Delta t)=x_{i-1}(t_0)$, $i=2,3,\ldots,M$,
   8.3. Update the γ matrix using Eqs. (24) and (25),
   8.4. Redistribute the number density according to Eq. (37),
   8.5. Set $t_0=\Delta t$, and $t_0=t_0+\Delta t$.
9. Else,
   9.1. Go to 10.
10. Go to step 5 until $t_0\geqslant t_f$.

Note that in step 8 if the equality is exactly satisfied, then $\boldsymbol{N}(t_0+\Delta t)=\boldsymbol{N}(t_0)$ except for the first interval where $N_1(t+\Delta t)=\gamma_1^{\langle 0\rangle}N_0(t)$.

9. Optimal fixed grid for droplet breakage in continuous systems

Unfortunately, the optimal moving grid technique developed in this work could not be applied in a straightforward manner to droplet breakage in continuous systems. The reason for this is the existence of two types of population densities in this type of systems. The first is the fixed droplet size distribution of the feed, $n^{\text{feed}}(v,t)$, and the second is that of droplets in the vessel itself $n(v,t)$. Since the droplet size distribution in the vessel moves continuously to the small size range with time, and the inlet feed size distribution is usually constant, the optimal maximum droplet size is fixed by that of the feed. Moreover, the optimal minimum droplet size in the vessel must be less than or equal to that of the feed. This leads to different grid widths for the droplet distribution in the vessel and in the feed where it becomes increasingly fine for the former and remains fixed for the latter. Mathematical inconsistencies are expected to occur due to integrating the terms involving $n(v,t)$ using a moving grid, while the feed term is integrated using the same grid at $t=0$. This is because the discrete number density, $N_i(t)$, is dependent on the size of the interval which is a function of time when a moving grid is used.

However, since droplet breakage in continuous systems is not expected to proceed to a very small size range as in the case of batch systems due to the fixed residence time of the vessel, an optimal fixed grid would be sufficient to minimize the total time-averaged FDE.

In the development of the moving grid technique for batch systems, we sought to minimize a total FDE based on the number density, FDE_0. However, there is still a FDE induced by excluding droplet volumes due to the failure of extending the domain of the internal coordinate to 0 and ∞. This is actually the total FDE based on the volume or the first moment of the distribution, and could be defined by an analogy to the zero FDE (Eq. (18)):

$$\varepsilon_1=\text{FDE}_1^L(v_{\min},t)+\text{FDE}_1^U(v_{\min},t), \tag{51}$$

where FDE_1^L and FDE_1^U are defined based on the first moment of the distribution by equations similar to Eqs. (14) and (15).

Since droplet breakage in batch systems leads to a population density that is skewed to the left, small volume of droplets are lost due to the failure of extending the droplet volume to infinity. However, for continuous systems the zero and first moments of the feed do affect the zero and first moments of the distribution in the vessel. Hence, where the feed distribution is constant as stated above, appreciable errors would result due to the exclusion of numbers and volumes from the domain. This marked influence of the feed density function on the moments of the distribution lends itself to consider both FDE based on the zero and first moments in seeking an optimal grid for discretization. In other words, we seek a grid that minimizes the time-average of the sum of the FDE based on both zero and first moments of the distribution. This total FDE is found by adding Eqs. (18) and (51) and the result could be related to the continuous zero and first moments of the distribution by analogy to Eq. (16):

$$\begin{aligned}M_0^d(v^*_{\min}(0),t)+M_1^d(v^*_{\min}(0),t)&\\ =M_0^c(t)+M_1^c(t)-[\varepsilon_0(v^*_{\min}(0),t)&\\ +\varepsilon_1(v^*_{\min}(0),t)].&\end{aligned} \tag{52}$$

Note that minimizing the total FDE (the term in square brackets) is equivalent to maximizing the sum of the left-hand side at any instant of time since the continuous zero and first moments of the distribution are functions of time only. Since the proposed optimal grid is fixed as mentioned above, it is recommended to maximize the time-average of the left-hand side of Eq. (52). The initial minimum droplet volume, $v^*_{\min}(0)$, could be obtained from the initial condition or from the feed droplet size distribution. Since $v^*_{\min}(0)$ is dependent on the interval width or σ for geometric grid, it is then $(M_0^d+M_1^d)$ is dependent only on the interval width or geometric factor σ at specified M. Thus, an optimal fixed grid is sought by finding the interval width or geometric factor that maximizes the time-average of $(M_0^d+M_1^d)$. In this work, we will restrict our attention to a geometric grid and thus, the problem at hand could be posed as a constrained one-dimensional

nonlinear optimization problem as follows:

$$\underset{\sigma}{\text{maximize}} \left(\frac{\int_0^{t_f} [M_0^d(\sigma,t) + M_1^d(\sigma,t)]}{t_f} \, \mathrm{d}t \right) \tag{53}$$

subject to:

$$\boldsymbol{N}(t) = \boldsymbol{R}\boldsymbol{D}\boldsymbol{R}^{-1}[\boldsymbol{N}(0) + \boldsymbol{A}^{-1}\boldsymbol{N}^{\text{feed}}] - \boldsymbol{A}^{-1}\boldsymbol{N}^{\text{feed}},$$

$$\frac{\mathrm{d}\boldsymbol{x}}{\mathrm{d}t} = \boldsymbol{F}(\boldsymbol{x},\boldsymbol{N}),$$

$$M_0^d(\sigma,t) + M_1^d(\sigma,t) = \boldsymbol{N}^{\mathrm{T}}(t)\boldsymbol{N}(t) + \boldsymbol{x}^{\mathrm{T}}(t)\boldsymbol{N}(t),$$

$$1 < \sigma \leqslant \sigma_{\max} \quad \text{for all } t \in [0, t_f].$$

where $\boldsymbol{N}^{\text{feed}}$ is an $M \times 1$ vector.

The above formulation minimizing the time-averaged total FDE has a distinctive feature by being dependent only on the chosen preserved properties of the distribution, which are already calculable from the solution of the DPBE themselves. The final time appearing in the system of Eqs. (53) is really the time at which the continuous system approaches steady state, which is a finite value and normally could be taken about 5τ for linear systems ($> 99\%$ of final steady state is achieved).

10. Numerical results

Although both the optimal moving and the fixed grids constructed in this work for minimizing the total FDE are general and applicable for any set of breakage functions, it is desirable to check thoroughly the numerical results by comparison with analytical solutions whenever it is possible. Two functional forms for both the daughter droplets distribution, $\beta(v \mid v')$, and breakage rate, $\Gamma(v)$, are used:

1. Uniform daughter droplet distribution, where it assumes an equal chance to form a daughter droplet of any smaller size when a mother droplet breaks up, and hence it is independent of daughter droplet volume (cases 1 and 2).
2. Parabolic daughter droplet distribution, where it assumes a more or less likely chance to form two daughter droplets of different sizes upon breakage of mother droplet (case 3).

The breakage rate function is assumed to have a general form:

$$\Gamma(v) = kv^m, \tag{54}$$

where k and m are positive parameters.

For the sake of comparison, available analytical solutions for droplet breakage in batch systems are presented in Table 2. Moreover, expressions are derived for the optimal minimum droplet volume, the continuous zero and first moments of the analytical distribution, and the total FDE. These are presented in Tables 3 and 4.

For the solution of droplet breakage in continuous systems, the problem of finding general analytical solutions becomes more difficult. However, two specific cases are presented in this work depending on the feed droplet distribution. In the first case McGrady and Ziff (1988) solved analytically the continuous PBE where a monodisperse feed droplet distribution is assumed. In the second case Nicmanis and Hounslow (1998) presented the steady-state solution of the continuous PBE with an exponential feed droplet distribution. However, for the dynamic solution, we extend the method of moments presented in the work of Vigil and Ziff (1989) for batch systems to continuous systems. Unfortunately, only the analytical zero and first moment of the distribution are obtained. In the following two sections, we first compare the numerical and the available analytical solutions for droplet breakage in batch systems, and finally the comparison is made for the continuous ones.

10.1. Droplet breakage in batch systems

In Table 2, we present three case studies to illustrate how the optimal moving grid works for the solution of droplet breakage in batch systems. In the first two cases a uniform daughter droplet distribution is assumed, while the exponent m in Eq. (54) is taken as 1 and 2, respectively. The initial droplet size distribution is exponential and the two cases along with their analytical solutions are shown in Table 2. The third case represents a more general parabolic daughter droplet distribution, however the analytical solution, to the best of the authors' knowledge, is not available. Nevertheless, the solutions using the fixed and optimal moving grid techniques will be compared. The comparison between the analytical and numerical results will be made on the bases of average number densities due to the sensitivity of the discrete number density to the interval width. Consequently, the average numerical and analytical discrete number densities are defined as

$$\bar{N}_i^{\text{num}} = \frac{N_i^{\text{num}}(t)}{\Delta v_i(t)}, \tag{55a}$$

$$\bar{N}_i^{\text{anal}} = \frac{N_i^{\text{anal}}(t)}{\Delta v_i(t)}. \tag{55b}$$

Note that the interval width is a function of time for an optimal moving grid and is time-invariant for the fixed one. Using the zero and first moments of the distribution the mean droplet volume is compared with the analytical solution using the following relation:

$$\bar{v}(t) = \frac{M_1^d(t)}{M_0^d(t)}. \tag{56}$$

Moreover, since wide differences in the average number density values are encountered as breakage progresses with time, a semi-log plot will be suitable for comparison. In this work, the number rather than the volume density is used to

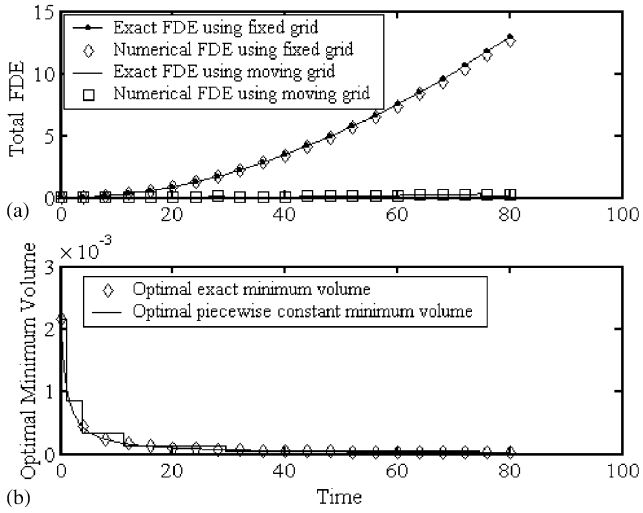

Fig. 2. (a) The effect of the optimal grid movement on the total FDE. (b) The approximate and exact optimal minimum droplet volume profiles for droplet breakage in a batch vessel using a geometric grid with factor $\sigma = 2.5$, $M = 10$, binary breakage, $\Gamma = v$, $\beta(v \mid \dot{v}) = 1/\dot{v}$, and exponential initial condition.

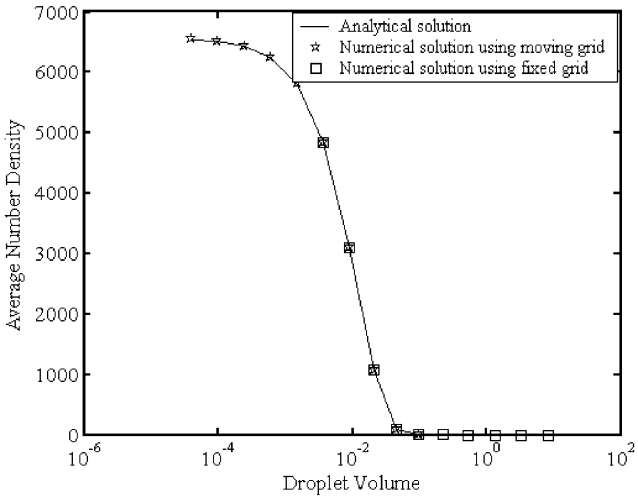

Fig. 3. The effect of the optimal grid movement on the average number density for droplet breakage in a batch vessel using a geometric grid with factor $\sigma = 2.5$, $M = 10$, binary breakage, $\Gamma = v$, $\beta(v \mid \dot{v}) = 1/\dot{v}$, exponential initial condition, and $t = 80$.

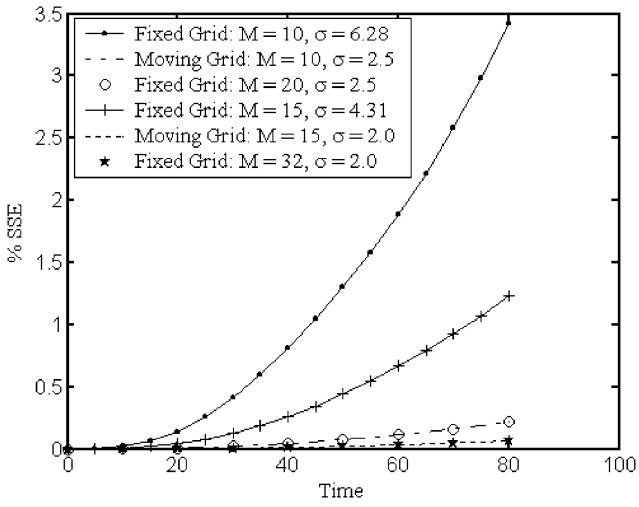

Fig. 4. The effect of the approximate optimal and fixed grids on the SSE using different levels of discretization for droplet breakage in a batch vessel with binary breakage, $\Gamma = v$, $\beta(v \mid \dot{v}) = 1/\dot{v}$, and exponential initial condition.

avoid damping the numerical errors, if any, where it actually occurs when a small droplet volume multiplies the number density particularly in the small size range. In all the case studies that follow arbitrary time units are used. Furthermore, all the simulation runs are carried out using the MATLAB software.

10.1.1. Case 1. Breakage with uniform daughter droplet distribution and $\Gamma(v) = v$

In this case (see Table 2), the simulation is carried out over a relatively long period of time, $t_f = 80$, to illustrate the steepness of the number density due to long time breakage. The solution algorithm is implemented for a number of intervals, $M = 10$, and $\sigma = 2.5$ to stress the use of a desirable relatively coarse geometric grid. We start this case by comparing the exact and numerical FDE as well as the optimal minimum droplet volumes. Fig. 2a shows these results, and it can be seen that an excellent agreement between the numerical and exact FDE is obtained. As expected, the optimal fixed FDE increases with time due to the failure to account for the increase in number density in the small size range as droplet breakage proceeds. This is actually equivalent to a loss of number of droplets from the system. To compensate for this, we let the grid move in an optimal manner as shown in Fig. 2b, where the exact minimum droplet volume (see Table 3) is depicted along with that predicted using the optimal moving grid technique. First the agreement between the optimal piecewise minimum droplet volume and the exact one is also good even when the grid moves so fast. Actually, the approximate profile is expected to approach the exact one as the number of pivots increases. The exact solution is obtained by inserting the analytical solution from Table 2 into Eq. (19). Second, the great influence of the optimal grid movement on the reduction of the total FDE is obvious when compared to the fixed grid (Fig. 2a). The exact solution is obtained by combining the analytical solution from Table 2 with Eq. (18).

Fig. 3 shows the exact and numerical average number densities at the final time of simulation where, excellent agreement is perceptible. Also, one could see how the optimal moving grid leaves the approximately empty intervals (large sizes) to accommodate the increasing number densities in the small size range as expected.

Fig. 4 depicts the sum of square errors (SSE), based on the difference between the exact and numerical solutions, as a function of time at different levels of discretization. The

Table 1
The CPU time requirements of the moving and fixed grids for droplet breakage in a batch vessel

Case	V_{min}	V_{M+1}	M	σ	% increase in the CPU time relative to case A	% Time averaged relative error in:	
						M_0	$\bar{V}$
A1: Fixed grid	2.16×10^{-7}	20.6	10	6.3	—	0.3000	0.0000
B1: Moving grid	$v^*_{min}(t)$	$v^*_{M+1}(t)$	10	2.5	3.59[a]	0.0976	0.0000
C1: Fixed grid	2.16×10^{-7}	20.6	20	2.5	39.88[a]	0.0976	0.0000
A2: Fixed grid	5.92×10^{-9}	19.4	15	4.3	—	0.1900	0.0000
B2: Moving grid	$v^*_{min}(t)$	$v^*_{M+1}(t)$	15	2.0	3.59[a]	0.0614	0.0000
C2: Fixed grid	5.92×10^{-9}	19.4	32	2.0	99.35[a]	0.0604	0.0000

[a]The CPU times are estimated under MATLAB 6.1 environment using a PC pentium II 700 MHz processor.

fixed and approximately optimal moving grids are compared such that the total FDE is negligible by extending the minimum and maximum droplet volumes to sufficiently small and large values (see Table 1). First grids of 10 pivots are used where it is clear that the fixed grid could cover the same domain spanned by the moving one only by having a geometric factor $\sigma = 6.28$. This relatively large geometric factor increases the error of integration with respect to v due to the large intervals width and hence the SSE increases as the distribution becomes sharp (after long breakage time). If the geometric factor is to be kept constant at $\sigma = 2.5$ for the fixed as well as the moving grids, then we need approximately 20 pivots for the fixed grid to have approximately the same SSE as the moving one. This will increase the computational time by about 40% when compared to case 1 (only 10 pivots) as is clear by referring to Table 1. This increase in the computational time is clearly due to the increase in the size of the system of ordinary differential equations (from 10 to 20). Similarly, if 15 pivots are used for both the fixed and moving grids the same trend is observed with the reduction of the SSE due to the small width of the intervals ($\sigma = 2$), and hence the integration error with respect to v. In this case the fixed grid requires approximately 32 pivots to cover the same domain spanned by the moving grid ($M = 15$) with relative increase in the CPU time about 100% (see Table 1). However, by referring to Table 1, the relative increase in the computational time in the case of the moving grid technique due to the redistribution algorithm is only about 3.6% in both cases. This clearly shows the effectiveness of the approximate optimal moving grid technique particularly for long time breakage.

Fig. 5 shows the optimal moving and fixed grids and their corresponding pivots at the end of the simulation time. It is clear that the positions of the moving and fixed pivots are approximately the same for the case of moving grids. This is because as the grid moves it becomes finer, and hence the moving pivots approaches the fixed ones, which agrees

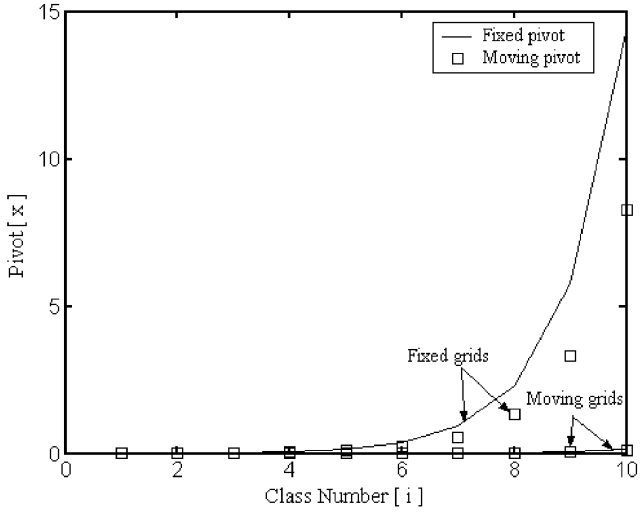

Fig. 5. The effect of the approximate optimal and fixed grids on the fixed and moving pivots at $t = 80$ using a geometric grid with factor $\sigma = 2.5$, $M = 10$ for droplet breakage in a batch vessel with binary breakage, $\Gamma = v$, $\beta(v \mid \hat{v}) = 1/\hat{v}$, and exponential initial condition.

with the condition implied by Eq. (49). However, in the case of the fixed grids with the same number of pivots, the fixed pivots are completely different from the moving ones particularly in the small size range due to the fixed width of the intervals as droplet breakage proceeds. This suggests that the solution of the PBE using the fixed pivot technique could be improved by using the present optimal moving grid.

10.1.2. Case 2. Breakage with uniform daughter droplet distribution and $\Gamma(v) = v^2$

In this case, the rate of droplet breakage is proportional to the square of its volume. A close look at the time constants given by $|\lambda_i^b|^{-1}$ $(i = 1, 2, \ldots, M)$ indicates that droplets with volume less than one will show slower dynamics when compared with that having the same volume in case 1. On the

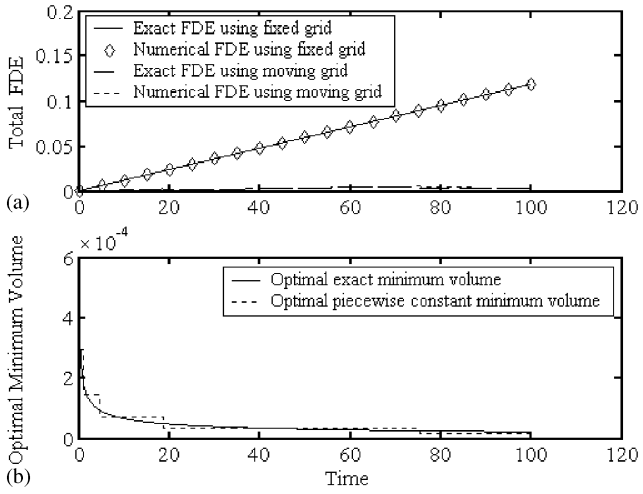

Fig. 6. (a) The effect of the optimal grid movement on the total FDE. (b) The approximate and exact optimal minimum droplet volume profiles for droplet breakage in a batch vessel using a geometric grid with factor $\sigma = 2$, $M = 15$, binary breakage, $\Gamma = v^2$, $\beta(v \mid \grave{v}) = 1/\grave{v}$, and exponential initial condition.

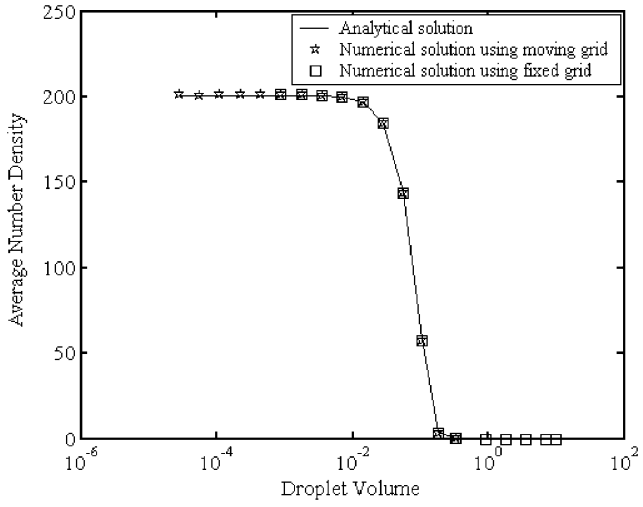

Fig. 7. The effect of the optimal grid movement on the average number density for droplet breakage in a batch vessel using a geometric grid with factor $\sigma = 2$, $M = 15$, binary breakage, $\Gamma = v^2$, $\beta(v \mid \grave{v}) = 1/\grave{v}$, and exponential initial condition.

contrary, droplets having volume greater than one will show faster dynamics when compared with that in case 1. Since the number density becomes skewed to the left as droplet breakage proceeds, slow dynamics will be dominant at long times. Due to this we have increased the simulation time to $t = 100$.

Fig. 6a shows how the optimal moving grid keeps the total FDE almost constant during the droplet breakage time. Moreover, the magnitude of the total FDE is considerably less than that in case 1 because of the nonsharply increasing number density with time at the small size range (see Fig. 7). As in case 1, it is clear from Fig. 6b that the optimal

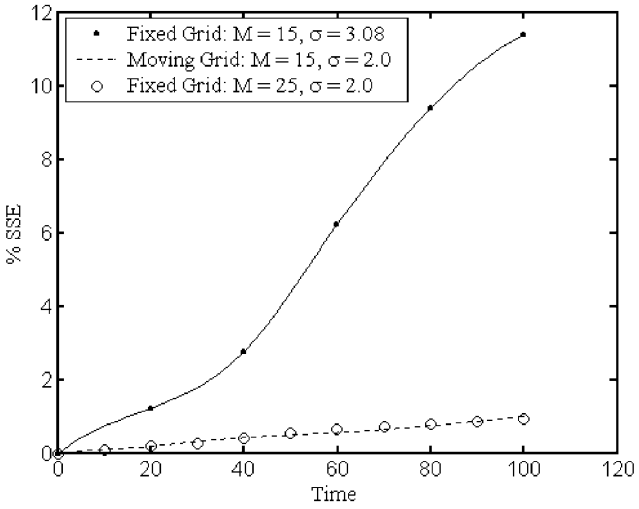

Fig. 8. The effect of the approximate optimal and fixed grids on the SSE using different levels of discretization for droplet breakage in a batch vessel with binary breakage, $\Gamma = v^2$, $\beta(v \mid \grave{v}) = 1/\grave{v}$, and exponential initial condition.

moving grid technique produces an optimal piecewise constant minimum droplet volume that is in a good agreement with the exact one given in Table 3.

Fig. 7 shows the expected average number density for the analytical (see Table 2) and numerical solutions at the end of the simulation time. Due to the slow and fast dynamics in the small and large size ranges, respectively; a sharp transition in the number density between these size ranges is encountered. Again it is evident how the approximate optimal moving grid leaves the almost empty intervals at the large size range to occupy the newly birthed population in the small size range.

Fig. 8 shows the behavior of the SSE as a function of time for this case using fixed and approximate optimal moving grids. The SSE using a fixed grid could only be reduced to that of the moving one ($M = 15$) only by increasing the number of pivots to 25 with the same geometric grid factor $\sigma = 2.0$. This will be at the expense of the computational time as is mentioned in case 1. In this case, the value of the SSE is greater than that of case 1 due to the increasing sharpness of the number density at the transition region from the large to the small size range.

10.1.3. Case 3. Breakage with parabolic daughter droplet distribution and $\Gamma(v) = v$

In this case, where parabolic daughter droplet distribution is assumed (Hill & Ng, 1995), we have added one different aspect being $\beta(v \mid v')$ is no longer independent of the daughter droplet volume. Since the analytical solution is not available, comparisons are made between the fixed and optimal moving grid techniques. Fig. 9a shows how the optimal moving grid reduces the total FDE and keeps it almost constant. The optimal piecewise constant minimum droplet volume is shown in Fig. 9b as is expected. The average number densities for both fixed and moving grids are depicted

Table 2
Available analytical solution for droplet breakage in batch systems

Case	$\beta(v \mid v')$	$\Gamma(v)$	$n(v,0)$	Analytical solution, $n(v,t)$	Reference
1	$\frac{2}{v'}$	v	e^{-v}	$(1+t)^2 e^{-v(1+t)}$	Ziff and McGrady (1985)
2	$\frac{2}{v'}$	v^2	e^{-v}	$[1+2t(1-v)]e^{(-tv^2-v)}$	Ziff and McGrady (1985)
3	$\frac{24(v^2-vv')+6v'^2}{v'^3}$	v	e^{-v}	Not available	Hill and Ng (1995)

Table 3
Analytical optimal minimum droplet volume, continuous zero and first moments, mean droplet volume, and the total FDE for droplet breakage in batch systems

Case	$v^*_{\min}(t)$	$M^c_0(t)$	$M^c_1(t)$	$\bar{v}^c(t)$	$\varepsilon_0(t)$
1	$\frac{(M-1)\ln(\sigma)}{(1+t)(\sigma^{M-1}-1)}$	$1+t$	1	$\frac{1}{1+t}$	$(1+t)\times(1+e^{-(1+t)v_{\max}}-e^{-(1+t)v_{\min}})$
2	$\frac{1+2t(1+v^*_{\min})}{1+2t(1+v^*_{\max})}$ $-\sigma^{M-1}\frac{e^{-(v^*_{\max}+v^{*2}_{\max}t)}}{e^{-(v^*_{\min}+v^{*2}_{\min}t)}}=0$	$1+\sqrt{\pi t}e^{1/4t}$ $\left[1-\mathrm{erf}\left(\frac{1}{2\sqrt{t}}\right)\right]$	1	$\frac{1}{M^c_0(t)}$	$(1+e^{-(v_{\max}+v^2_{\max}t)})$ $+\sqrt{\pi t}e^{1/4t}\times\left[1+\mathrm{erf}\left(\frac{2tv_{\min}+1}{2\sqrt{t}}\right)-\mathrm{erf}\left(\frac{2tv_{\max}+1}{2\sqrt{t}}\right)-\mathrm{erf}\left(\frac{1}{2\sqrt{t}}\right)\right]$
3	N.a.[a]	N.a.	1	N.a.	N.a.

[a]Not available.

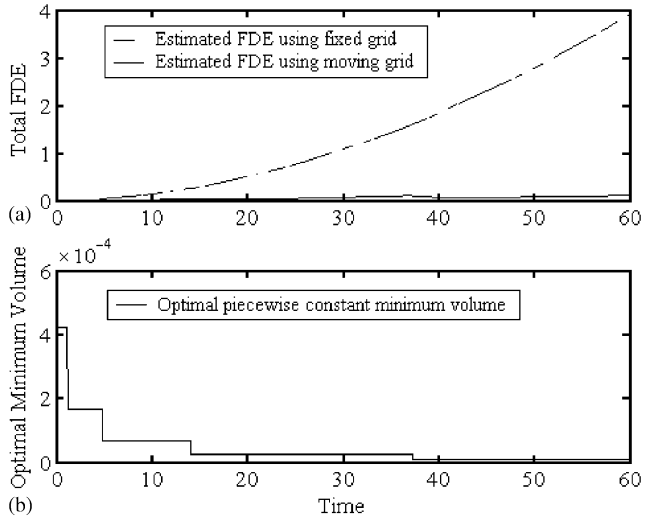

Fig. 9. (a) The effect of the optimal grid movement on the total FDE. (b) The approximate optimal minimum droplet volume profiles for droplet breakage in a batch vessel using a geometric grid with factor $\sigma = 2.5$, $M = 12$, binary breakage, $\Gamma = v$, $\beta(v \mid v') =$ parabolic, and exponential initial condition.

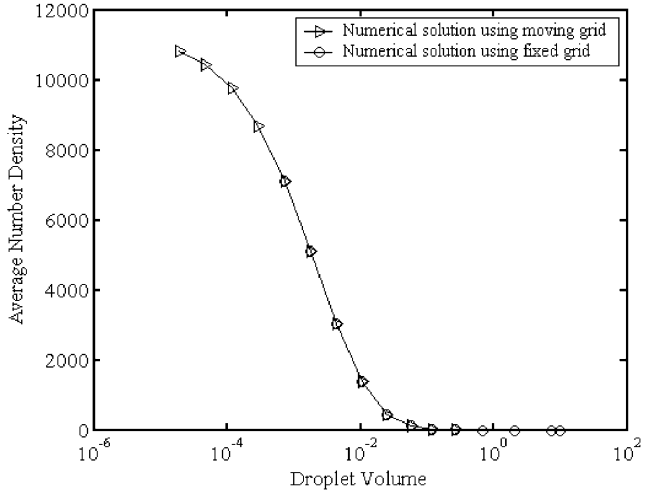

Fig. 10. The effect of the optimal grid movement on the average number density for droplet breakage in a batch vessel using a geometric grid with factor $\sigma = 2.5$, $M = 12$, binary breakage, $\Gamma = v$, $\beta(v \mid v') =$ parabolic, and exponential initial condition.

in Fig. 10 at the final simulation time. It is evident how the optimal moving grid follows the sharp part of the distribution while leaving the almost empty size intervals. All the desirable advantages achieved in cases 1 and 2 are retained in this case, which consolidate one's faith in the optimal moving grid technique.

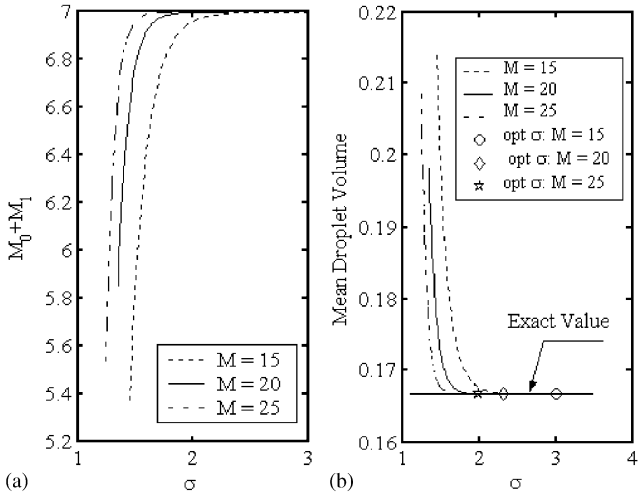

Fig. 11. Effect of the optimal geometric grid factor on: (a) The steady-state sum of zero and first moments of the distribution. (b) The mean droplet volume for droplet breakage in a continuous vessel with $\Gamma = v$ and $\beta(v \mid \grave{v}) = 1/\grave{v}$, binary breakage, $\tau = 5$, and exponential feed distribution.

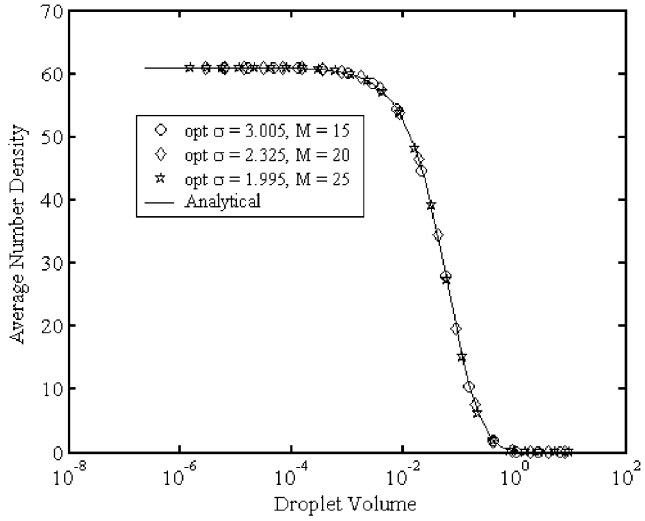

Fig. 12. Effect of the optimal geometric grid factor on the steady-state number density for droplet breakage in a continuous vessel with $\Gamma = v$ and $\beta(v \mid \grave{v}) = 1/\grave{v}$, binary breakage, $\tau = 5$, and exponential feed distribution.

10.2. Droplet breakage in continuous systems

In this section, optimal geometric factors (and hence optimal grids) are found for a given number of intervals by solving the constrained nonlinear optimization problem given by Eq. (53). The breakage functions considered are linear breakage rate ($k = 1, m = 1$) and uniform daughter droplet distribution for the two cases studied where zero initial conditions are assumed in the vessel. All the numerical simulations are conducted using MATLAB software.

10.2.1. Case 1. Exponential feed droplet distribution

In this case, the initial condition is assumed zero and the feed distribution is exponential. Table 4 shows the derived analytical solutions for the zero and first moments of the distribution, as well as the mean droplet volume for this special case. The optimization problem (Eq. (53)) is solved using three different levels of discretization ($M = 15, 20, 25$) to see their effect on the optimal geometric factor σ. The simulation time is chosen large enough (15τ) to insure that true final steady state is reached.

The initial optimal fixed grid used in the simulation is constructed using the feed droplet distribution and the optimal condition given by Eq. (19). The resulting geometric grid has the property of being expanded in both directions as σ increases to cover the lower and upper size ranges. This type of grid results in a monotone increasing function represented by the sum: $(M_0^d + M_1^d)$, since the number and volume densities increases monotonically as a result of simultaneous decrease and increase of $v_{\min}$ and $v_{\max}$, respectively. So, the optimal values of σ are the minimum ones which make the time-averaged $(M_0^d + M_1^d)$ constants to a prescribed accuracy. The numerical results are shown in Figs. 11 and 12. Fig. 11a shows the total zero and first moments of the distribution as function of the geometric factor at steady state. This figure shows three distinctive features: the first is the sharp decrease in the steady-state sum of the moments $(M_0^d + M_1^d)$ when the geometric factor is reduced below the optimal value, which is indeed equivalent to increasing the minimum droplet volume above the optimal one. This is equivalent to a sharp increase in the total FDE as it is evident from Eq. (52). This increase in the FDE is caused by the sharp increase in $v^*_{\min}(0)$ as a result of decreasing σ according to Eq. (19). The second feature is that the optimal geometric factor decreases as the number of intervals increases (Fig. 11b), which is expected since small geometric factor requires large number of intervals to cover the required discretized domain. The third feature is that all the steady-state values of $(M_0^d + M_1^d)$ are monotonically increasing where they become approximately identical and are slowly varying as the geometric factor is increased. This is again is attributed to the behavior of $v^*_{\min}(0)$, where it decreases sharply as σ increases resulting in negligible lower and upper residuals.

Fig. 11b shows the significant effect of the choice of the geometric factor on the mean droplet volume of the distribution. It is clear how the optimal values of σ result in an excellent prediction of the mean droplet volume. It is also evident that a small error in choosing σ below the optimal value will lead to significant error in the mean droplet volume due to the significant loss of droplet volumes and numbers from both boundaries.

Fig. 12 shows the average number density at steady state as predicted using three fixed grids with optimal geometric factors. The results show how the numerical solution is very close to the exact one at steady state at the three levels of discretization using optimal geometric grid factors. Fig. 13 shows an excellent agreement between the analytical and

Table 4
Mean droplet volume, zero and first moments of the distribution for droplet breakage in continuous systems

Case	$\beta(v \mid v')$	$\Gamma(v)$	$n^{\text{feed}}(v)$	$\bar{v}(t)$	$M_0(t)$	$M_1(t)$
1	$\frac{2}{v'}$	kv	e^{-v}	$\frac{M_1(t)}{M_0(t)}$	$c_2\tau(1-e^{-t/\tau})+(M_0(0)+c_1 t)e^{-t/\tau}$ $c_1 = k(M_1(0)-M_1^{\text{feed}})$ $c_2\tau = M_0^{\text{feed}} + kM_1^{\text{feed}}$	M_1^{feed} $+(M_1(0)-M_1^{\text{feed}})e^{-t/\tau}$
2	$\frac{2}{v'}$	kv	$\delta(v-x_f)$	$\frac{M_1(t)}{M_0(t)}$	$c_2\tau(1-e^{-t/\tau})+(M_0(0)+c_1 t)e^{-t/\tau}$ $c_1 = k(M_1(0)-\tau M_1^{\text{feed}})$ $c_2 = M_0^{\text{feed}} + k\tau M_1^{\text{feed}}$	$\tau M_1^{\text{feed}} + (M_1(0)-\tau M_1^{\text{feed}})e^{-t/\tau}$

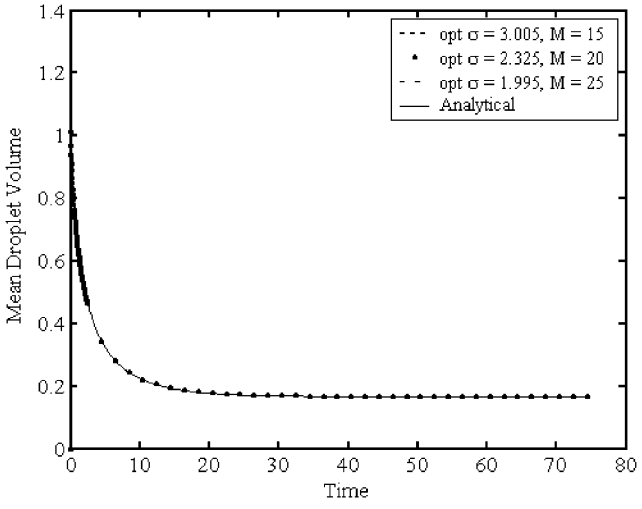

Fig. 13. Effect of the optimal geometric grid factor on the mean droplet volume for droplet breakage in a continuous vessel with $\Gamma = v$ and $\beta(v \mid \dot{v}) = 1/\dot{v}$, binary breakage, $\tau = 5$, and exponential feed distribution.

numerical mean droplet volumes even in the presence of the jump occurring at $t = 0$ due to the zero initial condition. Despite the small error involved in the predicted number densities at low level of discretization ($M = 15$), the numerical mean droplet volume is still in good agreement with the analytical one. This is natural since the present discretization technique preserves both total number and volume of the distribution.

10.2.2. Case 2. Monodisperse feed droplet distribution

In this case zero initial and monodisperse feed droplet distributions are used. The monodisperse feed distribution is mathematically represented by the Dirac delta function:

$$n^{\text{feed}}(v) = \delta(v - x_f). \tag{57}$$

McGrady and Ziff (1988) presented the analytical solution of a slight modified form of Eq. (1) for this case of droplet breakage in a continuous vessel. Table 4 shows the derived mean droplet volume, zero and first moments of the distribution. The discontinuous nature of the Dirac delta function imposes another difficulty when Eq. (57) is discretized. This function is approximated using the rectangular pulse function of unit area (Rice & Do, 1995; David, Villermaux, Marchal, & Klein, 1991):

$$N^{\text{feed}}(v - x_i) = \begin{cases} \dfrac{1}{\Delta v_f}, & v_f \leqslant v < v_{f+1}, \\ 0, & i \neq f, \end{cases} \tag{58}$$

where f is the index of the interval containing the feed droplet volume, x_f.

However, still another difficulty is imposed by Eq. (58) since the geometric grid which, is relatively coarse in the upper size range, makes the approximation above inaccurate. Introducing a linear grid to just encompass the interval containing the feed droplet size, x_f, alleviates this problem. The accuracy of the approximation is improved by making the linear grid as fine as required.

The system of Eqs. (53) is solved with ($x_f = 2.0$ as the maximum droplet volume) using three different levels of discretization to see how they affect the optimal gird geometric factor σ. The simulation results are shown in Figs. 14–16. In Fig. 14a, the steady state ($M_0^d + M_1^d$) are plotted against the grid geometric factor, where as in case 1, sharp increase in the total FDE results for those slightly below the optimal values. However, it is clear that above certain values of σ the steady state ($M_0^d + M_1^d$) becomes constant for the three levels of discretization used. This simply means that the upper residual of the distribution has a constant zero value, and hence the lower residual controls the total FDE. This result is not surprising, since the upper value of the droplet volume is bounded by the size of the monodisperse feed, x_f. Since the number density vanishes for all $v > x_f$, it follows then that the upper residual of the distribution is always zero provided that $v_{\max} \geqslant x_f$. In this case, the optimal values of σ are the minimum ones which make the time-averaged ($M_0^d + M_1^d$) constants to a prescribed accuracy and are shown in Fig. 14b. This case actually isolates the effect of the lower distribution residual and shows clearly that it is the dominant part contributing to the total FDE as long as pure droplet breakage is considered. As in case 1, the sensitivity of the total FDE to the changes of σ and its

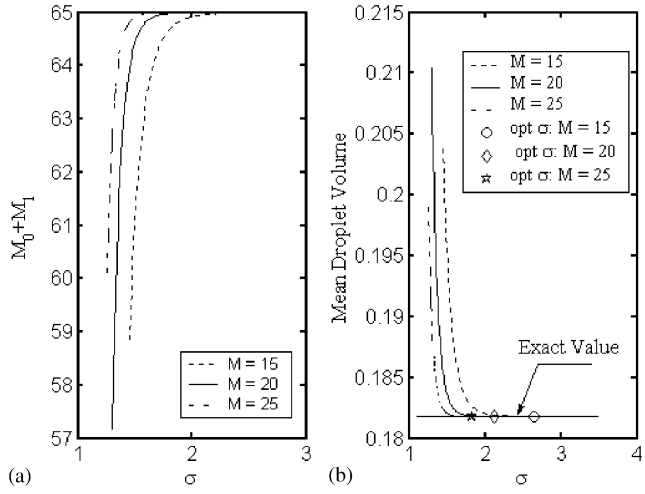

Fig. 14. Effect of the optimal geometric grid factor on: (a) The steady-state sum of zero and first moments of the distribution. (b) The mean droplet volume for droplet breakage in a continuous vessel with $\Gamma = v$, $\beta(v \mid \grave{v}) = 1/\grave{v}$, binary breakage, $\tau = 5$, and monodisperse feed distribution.

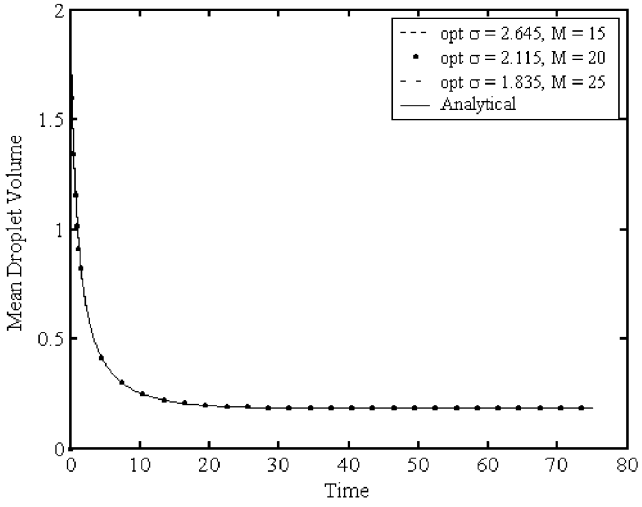

Fig. 16. Effect of the optimal geometric grid factor on the mean droplet volume for droplet breakage in a continuous vessel with $\Gamma = v$ and $\beta(v \mid \grave{v}) = 1/\grave{v}$, binary breakage, $\tau = 5$, and monodisperse feed distribution.

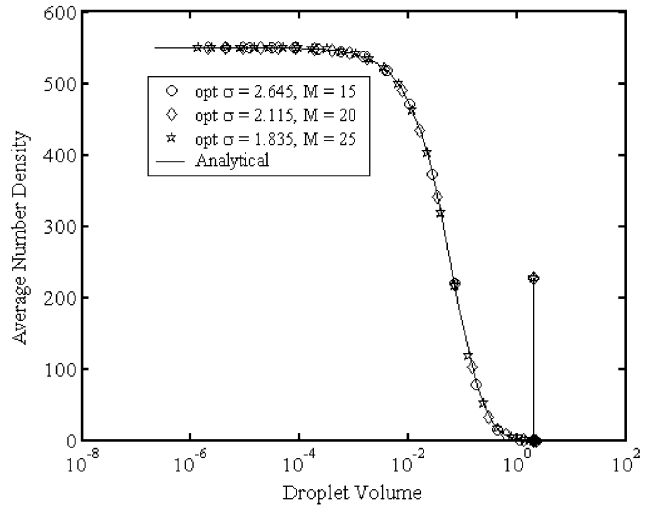

Fig. 15. Effect of the optimal geometric grid factor on the steady-state number density for droplet breakage in a continuous vessel with $\Gamma = v$ and $\beta(v \mid \grave{v}) = 1/\grave{v}$, binary breakage, $\tau = 5$, and monodisperse feed distribution.

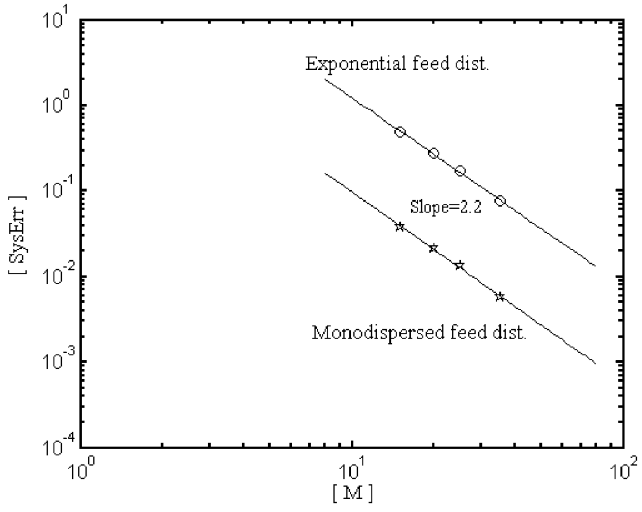

Fig. 17. The convergence characteristics of the moving pivot technique for droplet breakage in a continuous vessel with $\Gamma = v$ and $\beta(v \mid \grave{v}) = 1/\grave{v}$, binary breakage, and $\tau = 5$.

subsequence effect on the steady-state mean droplet volume is evident from Fig. 14b.

Fig. 15 shows the average number density at steady state as it is predicted along with the analytical solution using the optimal geometric grid factors shown in Fig. 14b. It is obvious that the agreement between the analytical and the numerical solutions is excellent. It is also worthwhile to see how the discontinuity in the number density is correctly predicted by using a fine linear grid around it. Fig. 16 shows how the predicted mean droplet volume is very close to the analytical one during the simulation time at different optimal geometric grid factors. To get more insight into the convergence characteristics of the numerical solutions presented in Figs. 12, 13, 15, and 16, it is helpful to define the systematic error (SysErr) as the absolute difference between the exact and the numerical mean droplet volumes:

$$\text{SysErr} = |\bar{v}_{\text{exac}} - \bar{v}_{\text{num}}|. \tag{59}$$

This is in fact a suitable choice since it involves both the conserved total number and volume of the droplet distribution. Fig. 17 shows the SysErr for both cases plotted on a log–log scale versus the number of pivots (intervals). The numerical solutions for both cases (monodisperse and exponential feed distributions) converge at the same rate due to the similar form of the distributions as it is evident from Figs. 12 and 15 where the slopes of both lines are equal to 2.2. This means that the moving pivot technique

converges at a rate that is inversely proportional to the square of the number of pivots ($\propto 1/M^2$). The magnitude of the SysErr for the case of the monodisperse feed distribution is smaller than that of the exponential one due to the effect of the total FDE. In the case of the monodisperse feed, $v_{max} = x_f$ and hence the upper residual is zero resulting in a bounded domain from the upper size range. This bounded domain makes the size of the intervals smaller than the case of the unbounded one for the exponential feed distribution and hence reduces the SysErr. This is actually reflected by comparing the values of the optimal geometric grid factors for both cases ($\sigma = 2.645$ for monodisperse and $\sigma = 3.005$ for exponential feed distributions when $M = 15$).

11. Conclusions

1. The moving pivot technique proposed by Kumar and Ramkrishna (1996b) is extended to continuous flow systems.
2. The slow movement of the pivots for sufficiently fine grid makes possible the sequential solution of the number density and the pivot equations in time.
3. Ordinary differential equations are derived to estimate the lower and upper residuals of the droplet distribution, which show excellent agreement with the analytical solutions studied in this work.
4. An approximate optimal moving grid technique is developed for droplet breakage in batch systems where the sharply increasing number density is successfully tracked out. The redistribution algorithm, on which this technique is based, is consistent with DPBEs by preserving any two integral properties of the distribution.
5. An optimal fixed grid that minimizes the time-averaged total FDE is also developed for continuous droplet breakage. This optimal grid represents a systematic approach for the determination of the minimum and maximum droplet volumes instead of the trial and error procedures that are usually used. The numerical results show that the lower residual of the distribution is dominant and makes the total FDE sensitive to small changes in the grid geometric factor.

Notation

$\boldsymbol{A}$	matrix for the number density equations as defined by Eq. (40)
$\boldsymbol{D}$	diagonal matrix whose elements are given by: $e^{\lambda_i^b t}$
$\boldsymbol{F}$	matrix for the pivot equations as defined by Eq. (41)
FDE_0^L	lower residual based on the zero moment of the distribution as defined by Eq. (14)
FDE_1^L	lower residual based on the first moment of the distribution
FDE_0^U	upper residual based on the zero moment of the distribution as defined by Eq. (15)
FDE_1^U	upper residual based on the first moment of the distribution
I_i	ith interval: $I_i = [v_i, v_{i+1})$
M	total number of intervals used in droplet volume discretization
M_0^c	zero moment of the continuous distribution
M_1^c	first moment of the continuous distribution
M_0^d	zero moment of the discrete distribution
M_1^d	first moment of the discrete distribution
$n(v,t)\,dv$	number of droplets in size range v to $v + dv$, at time t
$\boldsymbol{N}(t)$	vector whose ith component is the total number of droplets in the ith interval, at time t
$N_i(t)$	total number of droplets in the ith interval, at time t
N^{feed}	vector whose ith component is the total number of droplets in the ith interval for the feed
$\bar{N}_i^{anal}$	average discrete analytical number density in the ith interval defined by Eq. (55a)
$\bar{N}_i^{num}$	average discrete numerical number density in the ith interval defined by Eq. (55b)
$\bar{N}_i(t)$	average discrete number density in the ith interval at time t
$\boldsymbol{R}$	matrix whose columns are the eigenvectors of the matrix $\boldsymbol{A}$
SSE	sum of square of errors
t	time
t_0	initial simulation time
t_f	final simulation time
v, v'	droplet volumes
v_{min}, v_{max}	minimum and maximum droplet volumes
v_{min}^*, v_{max}^*	optimal minimum and maximum droplet volumes
$\bar{v}$	mean droplet volume
$\dot{v}$	droplet growth rate
$x_i(t)$	characteristic volume of the droplet population in the ith interval as defined by Eq. (4)

Greek letters

$\beta(v \mid v')\,dv$	fractional number of droplets formed in the size range v to $v + dv$ formed upon breakage of droplet of volume v'
δ	Dirac delta function
$\Delta v(t)$	width of the ith interval, $v_{i+1} - v_i$, at time t
$\varepsilon_0(t)$	total finite domain error based on zero moment of the distribution as defined by Eq. (18) (error of discretization)
$\varepsilon_1(t)$	total finite domain error based on first moment of the distribution as defined by Eq. (51) (error of discretization)
η_i	the ith eigenvalue of the matrix $\boldsymbol{F}$ as defined by Eq. (11)

$\gamma_i^{\langle i \rangle}$	fraction of droplets at the pivot $x_i(t)$ that is assigned to the pivot $x_i(t+\Delta t)$ in the ith interval
$\Gamma(v)$	number of droplets in the size range v to $v+\mathrm{d}v$ disappearing per unit time by breakage
λ_i^b	the ith eigenvalue of the matrix $\boldsymbol{A}$ for batch droplet breakage
λ_i^c	the ith eigenvalue of the matrix $\boldsymbol{A}$ as defined by Eq. (9) for continuous droplet breakage
$\omega(v,v')$	coalescence frequency between two droplets of volumes v and v'
$\pi_{0,i,k}$	as defined by Eq. (8)
$\pi_{1,i,k}$	as defined by Eq. (12)
σ	geometric grid factor
τ	vessel residence time
$\vartheta(v')$	average number of droplets produced when mother droplet of volume, v', is broken

Acknowledgements

The authors wish to thank the DAAD STIBET matching fund to support this work.

References

Alopaeus, V., Koskinen, J., & Keskinen, K. I. (1999). Simulation of population balances for liquid–liquid systems in a nonideal stirred tank. Part 1. Description and qualitative validation of model. *Chemical Engineering Science*, *54*, 5887–5899.

Bajpai, R. K., & Ramkrishna, D. (1976). A coalescence redispersion model for drop-size distribution in an agitated vessel. *Chemical Engineering Science*, *31*, 913–920.

Barone, J. P., Furth, W., & Loynaz, S. (1980). Simplified derivation of the general population balance equation for a seeded, continuous flow crystallizer. *Canadian Journal of Chemical Engineering*, *58*, 137–138.

Blatz, P. J., & Tobolsky, A. V. (1945). Note on the kinetics of systems manifesting simultaneous polymerization–depolymerization phenomena. *Journal of Physical Chemistry*, *49*, 77–80.

Bleck, R. (1970). A fast, approximate method for integrating the stochastic coalescence equation. *Journal of Geophysical Research*, *75*, 5165–5171.

David, R., Villermaux, J., Marchal, P., & Klein, J. P. (1991). Crystallization and precipitation engineering—IV. Kinetic model of adipic acid crystallization. *Chemical Engineering Science*, *46*, 1129–1136.

Eid, K., Gourdon, C., & Casamatta, G. (1991). Drop breakage in a pulsed sieve-plate column. *Chemical Engineering Science*, *46*, 1595–1608.

Garg, M. O., & Pratt, H. R. C. (1984). Measurement and modeling of droplet coalescence and breakage in a pulsed plate extraction column. *A.I.Ch.E. Journal*, *30*, 432–441.

Gelbard, F., & Seinfeld, J. H. (1978). Numerical solution of the dynamic equation for particulate systems. *Journal of Computational Physics*, *28*, 357–375.

Gerald, C. F., & Wheatly, P. O. (1994). *Applied numerical analysis* (5th ed.). New York: Addison-Wesley.

Hill, P. J., & Ng, K. M. (1995). New discretization procedure for the breakage equation. *A.I.Ch.E. Journal*, *41*, 1204–1216.

Hounslow, M. J. (1990). A discretized population balance for continuous systems at steady state. *A.I.Ch.E. Journal*, *36*, 106–116.

Hounslow, M. J., Ryall, R. L., & Marshall, V. R. (1988). A discretized population balance for nucleation, growth, and aggregation. *A.I.Ch.E. Journal*, *34*, 1821–1832.

Kostoglou, M., & Karabelas, A. J. (1994). Evaluation of zero order methods for simulating particle coagulation. *Journal of Colloid and Interface Science*, *163*, 420–431.

Kumar, S., Kumar, R., & Gandhi, K. S. (1993). A new model for coalescence efficiency of drops in stirred dispersions. *Chemical Engineering Science*, *48*, 2025–2038.

Kumar, S., & Ramkrishna, D. (1996a). On the solution of population balance equations by discretization—I. A fixed pivot technique. *Chemical Engineering Science*, *51*, 1311–1332.

Kumar, S., & Ramkrishna, D. (1996b). On the solution of population balance equations by discretization—II. A moving pivot technique. *Chemical Engineering Science*, *51*, 1333–1342.

Kumar, S., & Ramkrishna, D. (1997). On the solution of population balance equations by discretization—III. Nucleation, growth and aggregation of particles. *Chemical Engineering Science*, *52*, 4659–4679.

Laso, M., Steiner, L., & Hartland, S. (1987). Dynamic simulation of liquid–liquid agitated dispersions—I. Derivation of a simplified model. *Chemical Engineering Science*, *42*, 2429–2436.

Lister, J. D., Smit, D. J., & Hounslow, M. J. (1995). Adjustable discretized population balance for growth and aggregation. *A.I.Ch.E. Journal*, *41*, 591–603.

Marchal, P., David, R., Klein, J. P., & Villermaux, J. (1988). Crystallization and precipitation engineering—I. An efficient method for solving population balance in crystallization with agglomeration. *Chemical Engineering Science*, *43*, 59–67.

McGrady, E. D., & Ziff, R. M. (1988). Analytical solutions to fragmentation equation with flow. *A.I.Ch.E. Journal*, *34*, 2073–2076.

Mickley, H. S., Sherwood, T. S., & Reed, C. E. (1990). *Applied mathematics in chemical engineering*. New Delhi: McGraw-Hill.

Milton, J. S., & Arnold, J. C. (1990). *Introduction to probability and statistics* (2nd ed.). New York: McGraw-Hill.

Nicmanis, M., & Hounslow, M. J. (1998). Finite-element methods for steady-state population balance equations. *A.I.Ch.E. Journal*, *44*, 2258–2272.

Podgorska, W., & Baldyga, J. (2001). Scale-up effects on the drop size distribution of liquid–liquid dispersions in agitated vessels. *Chemical Engineering Science*, *56*, 741–746.

Ramkrishna, D. (1985). The status of population balances. *Reviews of Chemical Engineering*, *3*, 49–95.

Ramkrishna, D. (2000). *Population balances*. San Diego: Academic Press.

Ribeiro, L. M., Regueiras, P. F. R., Guimaraes, M. M. L., Madureira, C. M. C., & Cruz-Pintu, J. J. C. (1995). The dynamic behavior of liquid–liquid agitated dispersions—I. The hydrodynamics. *Computers in Chemical Engineering*, *19*, 333–344.

Rice, G. R., & Do, D. D. (1995). *Applied mathematics and modeling for chemical engineers*. New York: Wiley.

Scott, W. T. (1968). Analytical studies in cloud droplet coalescence I. *Journal of Atmospheric Science*, *25*, 54–65.

Sovova, H., & Prochazka, J. (1981). Breakage and coalescence of drops in a batch stirred vessel—I. Comparison of continuous and discrete models. *Chemical Engineering Science*, *36*, 163–171.

Tsouris, C., & Tavlarides, L. L. (1994). Breakage and coalescence models for drops in turbulent dispersions. *A.I.Ch.E. Journal*, *40*, 395–406.

Valentas, K. J., & Amundson, A. R. (1966). Breakage and coalescence in dispersed phase systems. *Industrial and Engineering Chemistry Fundamentals*, *5*, 533–542.

Valentas, K. J., Bilois, O., & Amundson, A. R. (1966). Analysis of breakage in dispersed phase systems. *Industrial and Engineering Chemistry Fundamentals*, *5*, 271–279.

Vigil, R. D., & Ziff, R. M. (1989). On the stability of coagulation-fragmentation population balances. *Journal of Colloid and Interface Science*, *133*, 257–264.

Ziff, R. M. (1991). New solutions to the fragmentation equation. *Journal of Physics A: General Physics*, *24*, 2821–2828.

Ziff, R. M., & McGrady, E. D. (1985). The kinetics of cluster fragmentation and depolymerisation. *Journal of Physics A: General Physics 18*, 3027–3037.